31. HISTORY OF THE WALVIS RIDGE[1]

T. C. Moore, Jr.,[2] P. D. Rabinowitz,[3] P. E. Borella,[4] N. J. Shackleton,[5] and A. Boersma[6]

ABSTRACT

Five sites were drilled along a transect of the Walvis Ridge. The basement rocks range in age from 69 to 71 Ma; the deeper sites are slightly younger, in agreement with the seafloor-spreading magnetic lineations. Geophysical and petrological evidence indicates that the Walvis Ridge was formed at a mid-ocean ridge at anomalously shallow elevations. The basement complex associated with the relatively smooth acoustic basement in the area consists of pillowed basalt and massive flows alternating with nannofossil chalk and limestone that contain a significant volcanogenic component. Basalts are quartz tholeiites at the ridge crest and olivine tholeiites downslope. The sediment sections are dominated by carbonate oozes and chalks; volcanogenic material, probably derived from sources on the Walvis Ridge, is common in the lower parts of the sediment columns.

Paleodepth estimates based on the benthic fauna are consistent with a normal crustal-cooling rate of subsidence of the Walvis Ridge. The shoalest site in the transect sank below sea level in the late Paleocene, and benthic fauna indicate a rapid lowering of the sea level in the mid-Oligocene.

Average accumulation rates during the Cenozoic indicate three peaks in the rate of supply of carbonate to the seafloor: early Pliocene, late middle Miocene, and late Paleocene to early Eocene. Carbonate accumulation rates for the rest of the Cenozoic averaged 1 g/cm^2 per 10^3 y. Dissolution had a marked effect on sediment accumulation in the deeper sites, particularly during the late Miocene, Oligocene, and middle to late Eocene. Changes in accumulation rates with depth indicate that the upper part of the water column had a greater degree of undersaturation with respect to carbonate during times of high productivity. Even when the CCD was below 4400 m, a significant amount of carbonate was dissolved at the shallower sites.

The flora and fauna of the Walvis Ridge are temperate in nature. Warmer water faunas are found in the uppermost Maestrichtian and lower Eocene sediments; cooler water faunas are present in the lower Paleocene, Oligocene, and middle Miocene. The boreal elements of the lower Pliocene are replaced by more temperate forms in the middle Pliocene.

The Cretaceous/Tertiary boundary was recovered in four sites; the sediments contain well-preserved nannofossils but poorly preserved foraminifers.

INTRODUCTION

The drilling plan for Leg 74 of the Deep Sea Drilling Project was designed to address three main scientific problems: (1) the history of the deep water circulation in the southeastern Atlantic; (2) the nature and geologic evolution of the Walvis Ridge; and (3) the biostratigraphy and magnetic stratigraphy of this region. In order to study these problems, five sites were drilled on the Walvis Ridge in June and July 1980 (Fig. 1; Table 1), extending from its crest (near 1000 m water depth) down its northwestern flank into the Angola Basin to a depth of 4400 m.

The sites are relatively closely spaced, encompassing a northwest–southeast transect of approximately 230 km. They span a water depth range of over 3 km, and receive approximately the same rain of pelagic debris. Any differences among sites in average accumulation rates for a given interval of time should result from two main processes: (1) differences in dissolution rate as a function of depth, and (2) differences in winnowing and erosion, which may also vary as a function of depth and are likely to be important near large topographic features. Detailed stratigraphic studies and the analysis of the accumulation rates for components of different sizes aid in distinguishing these two processes.

The classical marine biostratigraphies have been largely established in tropical sequences (Bolli, 1957; Blow, 1969; Berggren, 1972). The Walvis Ridge transect should help establish biostratigraphies in more temperate latitudes. The usefulness of this material is enhanced by the recovery of several sections within a relatively small geographic area and by the use of the Hydraulic Piston Corer (HPC) in three of the five sites. The HPC is capable of recovering relatively undisturbed sedimentary sections and thus provides the opportunity for detailed studies of biostratigraphy, paleomagnetism, physical properties, and other biological and geological parameters. Complete coring of several sites within a small area assures nearly complete recovery of the biostratigraphic sequence and optimal preservation of both older and younger parts of the section—the former in deeper sites with less overburden and diagenesis and the latter in shoaler sites with less dissolution.

The study of the evolution of the Walvis Ridge is also aided by this transect of sites. First, the transect allows us to date the age and subsidence history of the ridge. Second, the basement samples allow us to study the magnetic character, petrology, and chemical composition of the crustal rocks as well as the mode of emplacement of the basement complex.
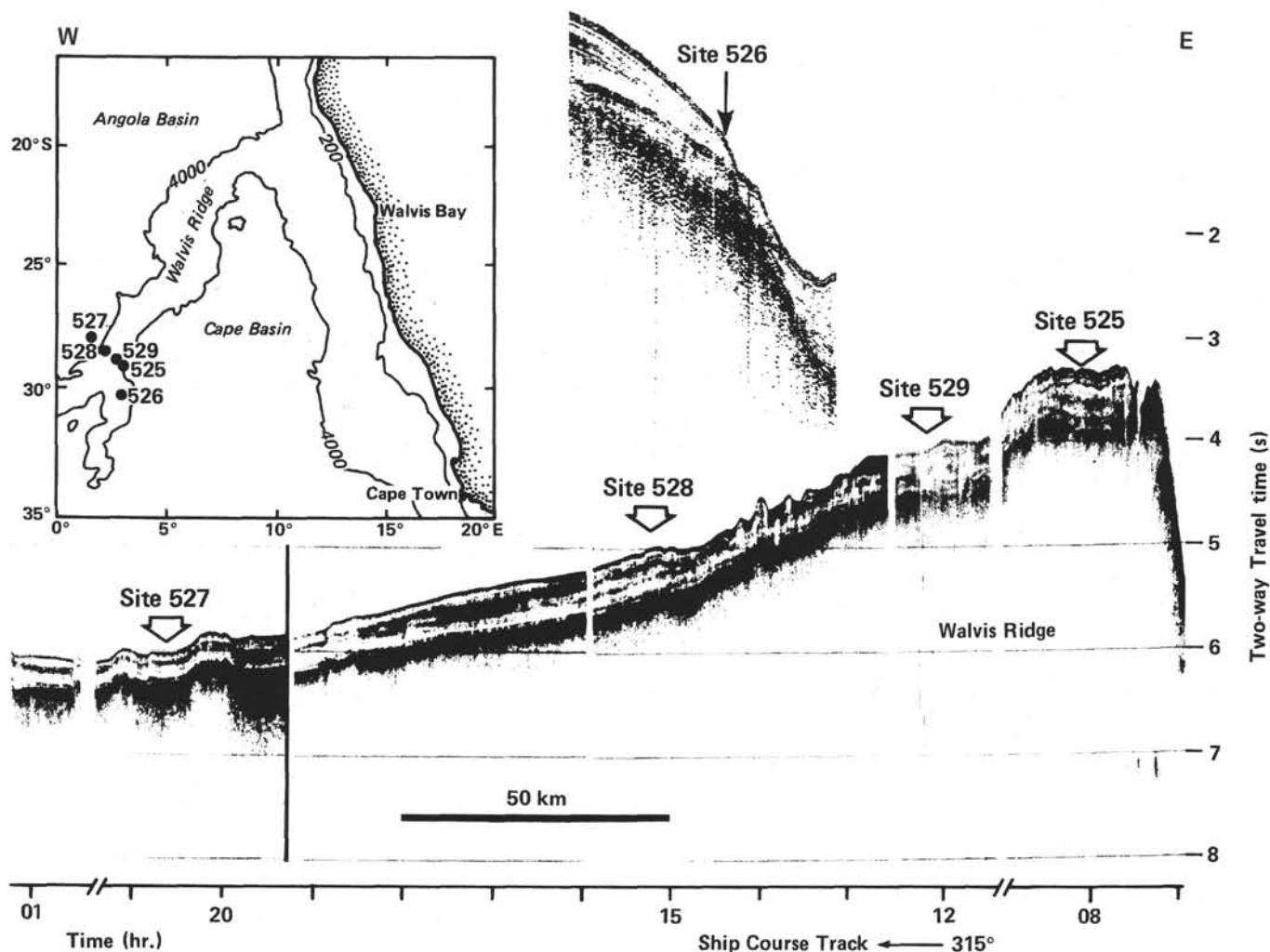
Figure 1. Site localities and index map.

Table 1. Leg 74 coring summary.

Hole	Latitude	Longitude	Water Depth (m below sea level)	Penetration	No. Cores	Meters Cored	Meters Recovered	Recovery (%)
525	29°04.24′S	02°59.12′E	2467 m	3.6 m	1	3.6	3.6	100
525A	29°04.24′S	02°59.12′E	2467 m	678.1 m	63	555.1	406.7	73
525B	29°04.24′S	02°59.12′E	2467 m	285.6 m	53	227.0	181.7	80
526	30°07.36′S	03°08.28′E	1054 m	6.3 m	2	6.3	3.6	57
526A	30°07.36′S	03°08.28′E	1054 m	228.8 m	46	200.8	206.6	100+
526B	30°07.36′S	03°08.28′E	1054 m	28.3 m	5	22.0	13.5	61
526C	30°07.36′S	03°08.28′E	1054 m	356.0 m	21	185.0	70.9	38
527	28°02.49′S	01°45.80′E	4428 m	384.5 m	44	384.5	243.9	63
528	28°31.49′S	02°19.44′E	3800 m	555.0 m	47	441.0	272.8	62
528A	28°31.16′S	02°18.97′E	3815 m	130.5 m	30	130.5	116.5	89
529	28°55.83′S	02°46.08′E	3035 m	417.0 m	44	417.0	309.7	74
Total					356	2572.8	1829.5	71

OCEANOGRAPHIC SETTING

All sites lie beneath the generally northward-flowing surface currents in the eastern part of the central subtropical gyre, and are approximately 800 km off the coast of Africa, well outside the main flow of the eastern boundary current (Benguela Current) and the associated regions of high productivity. With the possible exception of storm-induced currents, near-surface conditions are rather uniform over the study area and are assumed to have remained so in the past. Even if surface current patterns changed significantly in the past, at any

given time all sites within this relatively small study area probably received a nearly uniform supply of biogenic and detrital material.

All sites are above the 5 km-deep calcium carbonate lysocline, the depth at which the dissolution rate rapidly increases, in this region. Only Sites 527 and 528 lie near the level of "perceptible dissolution" (R_o level of Berger, 1977) or the calcite saturation level of Takahashi (1975), both of which are thought to be near 4 km in the southeastern Atlantic. The shallowest site (526, at 1054 m) lies within the depth interval presently occupied by Antarctic Intermediate Waters (AAIW). The remaining deeper sites are located at depths ranging from approximately 2500 to 4400 m (Table 1), well within the depth interval occupied by the North Atlantic Deep Water (NADW), which presently dominates the deep and bottom waters of the Angola Basin. The Walvis and Mid-Atlantic ridges form an effective topographic barrier which largely isolates the Angola Basin from the strong dissolution effects of chemically "older" Antarctic Bottom Water (AABW) (higher in dissolved CO_2 and nutrients) to the south and west. Only a small amount of AABW enters the Angola Basin through the two deepest passages: the Romanche Fracture Zone located near the equator (Wust, 1936) and the Walvis Passage located near the southwestern end (36°S, 7°W) of the Walvis Ridge (Connary and Ewing, 1974). Geologic evidence from previous Deep Sea Drilling Project legs (Maxwell, Von Herzen et al., 1970; Bolli, Ryan, et al., 1978; Hsü and LaBrecque, in press) suggests that the chemical character of the deep and bottom water of the Angola Basin has changed markedly through the Cenozoic.

GEOLOGIC SETTING

The Walvis Ridge consists of offset north-northwest-trending crustal blocks, connected by east-northeast-trending blocks. Together these segments form a roughly linear ridge which extends to the northeast from the Mid-Atlantic Ridge and joins the continental margin of Africa near 20°S latitude. Within the area of study (Figs. 1 and 2), structural blocks tend to slope steeply toward the Cape Basin and more gradually northwestward toward the Angola Basin.

Until recently it was uncertain whether or not the Walvis Ridge was an oceanic crustal feature or a fragment of continental crust which was separated from the main continental blocks during the early phases of rifting in the South Atlantic. Seismological and gravity studies indicate that the average crustal thickness beneath the ridge is 12 to 15 km and that the seismic character of the crust is consistent with an oceanic origin (Chave, 1979; Detrick and Watts, 1979; Goslin and Sibuet, 1975). Previous investigations suggest that part of the Walvis Ridge may be a manifestation of an oceanic hot spot (Morgan, 1971, 1972; Wilson, 1963; Burke and Wilson, 1976). Other investigations have shown that ridge crest migrations have played an important role in the evolution of this part of the South Atlantic Ocean (Rabinowitz and LaBrecque, 1979). Magnetic data from a recent geophysical survey of the study area (Rabinowitz and

Simpson, 1979) are interpreted as Magnetic Anomaly 32 (lower Maestrichtian) on the crest of the Walvis Ridge, with younger anomalies extending to the west into the Angola Basin (see Fig. 2). These results lend support to the idea that the Walvis Ridge was formed at a mid-ocean ridge by seafloor spreading processes.

Site 526, the shoalest site, lies near the crest of what appears to be a separate structural block, to the south of the block on which the remaining four sites in the transect were drilled (Figs. 1 and 2). Site 525 is located near the crest of the more northern block, in an area having nearly 600 m of sediment. Site 529, the next deeper site, lies on the eastern flank of a valley which forms a saddle in the ridge. Sites 528 and 527 are in progressively deeper waters and have somewhat thinner sedimentary sections.

Acoustic basement in the study area is comparatively smooth; pronounced basement highs are found most commonly in the crestal regions. There appear to be at least three sub-bottom acoustic reflectors on seismic profiles; these reflectors define four sedimentary intervals which can be traced through the area. The section beneath the deepest sediment reflector thins downslope and nearly merges with the basement reflector in the area of Site 527 (Fig. 1). The next shoaler interval appears to be of approximately constant thickness throughout the transect, whereas the one above that (third from the bottom) appears to pinch-out between Sites 528 and 527. The shoalest interval is dissected between Sites 529 and 528 and thins between Sites 528 and 527. Evidence of erosion and slumping in the study area is seen in the reflection records taken near the edges of the crestal region and near the valley to the west of Sites 525 and 529.

Sediments of the study area are composed mainly of calcareous oozes ($> 90\%$ $CaCO_3$). Because NADW predominates in most of the Angola Basin, the calcite compensation depth presently lies below 5500 m (Berger and Winterer, 1974). The noncarbonate fraction is dominated by clay with very little or no biogenic opal.

DRILLING RESULTS

Site Summaries

In the following paragraphs the sediment and basement lithologies are summarized in order of depth of site along the transect (shallow to deep). The details of the cores recovered, sediment classification, physical properties, and chemical and analytical techniques used can be found in the site chapters.

Site 526 on crust of Anomaly 31–32 age (mid-Maestrichtian to late Campanian) is the shallowest site, drilled with the primary objective of recovering a relatively complete and well-preserved Neogene and upper Paleocene calcareous sedimentary section (Fig. 3). The site was piston-cored to a sub-bottom depth of 229 m (Holes 526, 526A, and 526B) with a recovery rate of 98%. We rotary-cored to 356 m sub-bottom (Hole 526C) and the recovery rate averaged 38% before the hole was terminated when we encountered a thick, poorly lithified sandstone formation which created unstable hole conditions.
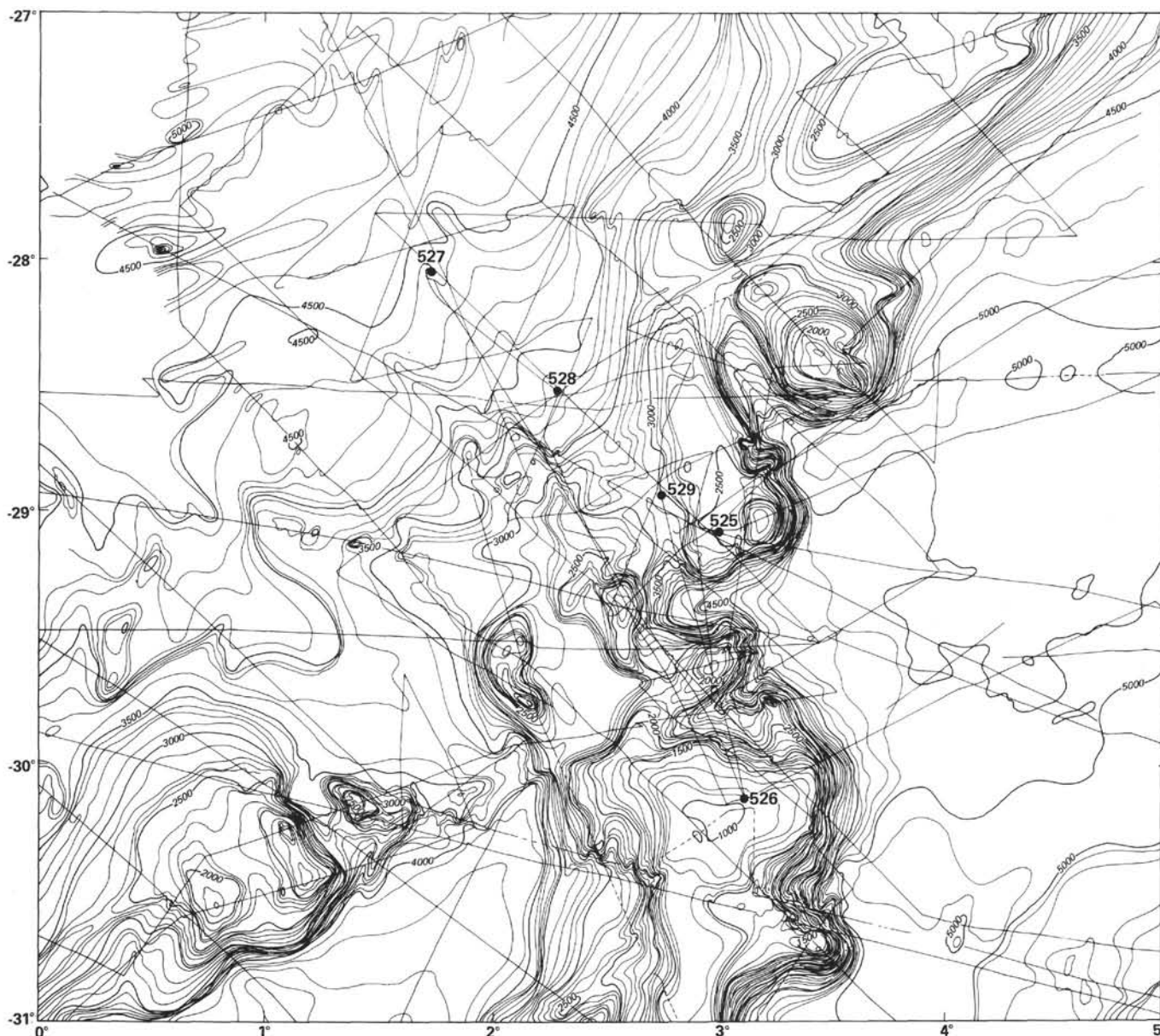
-Figure 2. Bathymetry of Walvis Ridge. Tracklines shown are those of *Thomas B. Davie.*

Five major lithologic units (Fig. 3) are observed:

Unit I, from the mud line (Recent) to about 130 m sub-bottom (lower Miocene), consists of a very homogeneous white foraminiferal–nannofossil ooze. Bioturbation is common. Carbonate content is ~97%.

Unit II, from 130 to ~195 m sub-bottom (lower Oligocene) is a homogeneous, very pale orange to pinkish gray nannofossil ooze with minor chalk layers. Bioturbation is slight. Carbonate content is ~95%.

Unit III, from 195 to about 225 m sub-bottom (upper Eocene) is a homogeneous, pinkish gray, foraminiferal–nannofossil ooze. No biogenic sedimentary structures are observed. Carbonate content is ~95%.

Unit IV, from 225 to 242 m (upper Eocene) is a thin, white, rubbly, limestone layer containing oncoliths and large oyster shells. The limestone rubble is graded and probably represents a channel fill.

Unit V, from ~242 to 356 m sub-bottom (upper Paleocene) is a poorly lithified, calcareous sandstone with debris of bryozoans and shell fragments of lamellibranchs and echinoids, indicating very shallow water conditions. Acoustic volcanic basement was not penetrated at this site.

Site 525 on crust of Magnetic Anomaly 32 age (early Maestrichtian–late Campanian) is located on a broad,

relatively flat crest of a block of the Walvis Ridge that trends north-northeast and south-southwest. Three holes (Fig. 4) give a complete section from the seafloor to the top of a basement complex at 574 m sub-bottom. An additional 103 m were drilled into the basement complex, for a total penetration of 677 m.

Four major sedimentary lithologic units are observed:

Unit I, consists of a very homogeneous nannofossil and foraminiferal–nannofossil ooze. The base of Unit I coincides with a color change and major hiatus between upper Oligocene and middle Eocene at 270 m sub-bottom.

Unit II, consists of nannofossil and foraminiferal–nannofossil oozes and chalks which terminate in the lower Paleocene at about 445 m sub-bottom. Chert fragments were found near the base of Unit II. Carbonate content in Units I and II is generally greater than 90%.

Unit III, sediments extend from the lower Paleocene to the basement complex at 574 m sub-bottom and consist of a cyclical pattern of nannofossil marly chalks and siltstones/sandstones of turbidite and/or slump origin. Included in the unit is the Cretaceous/Tertiary bound-

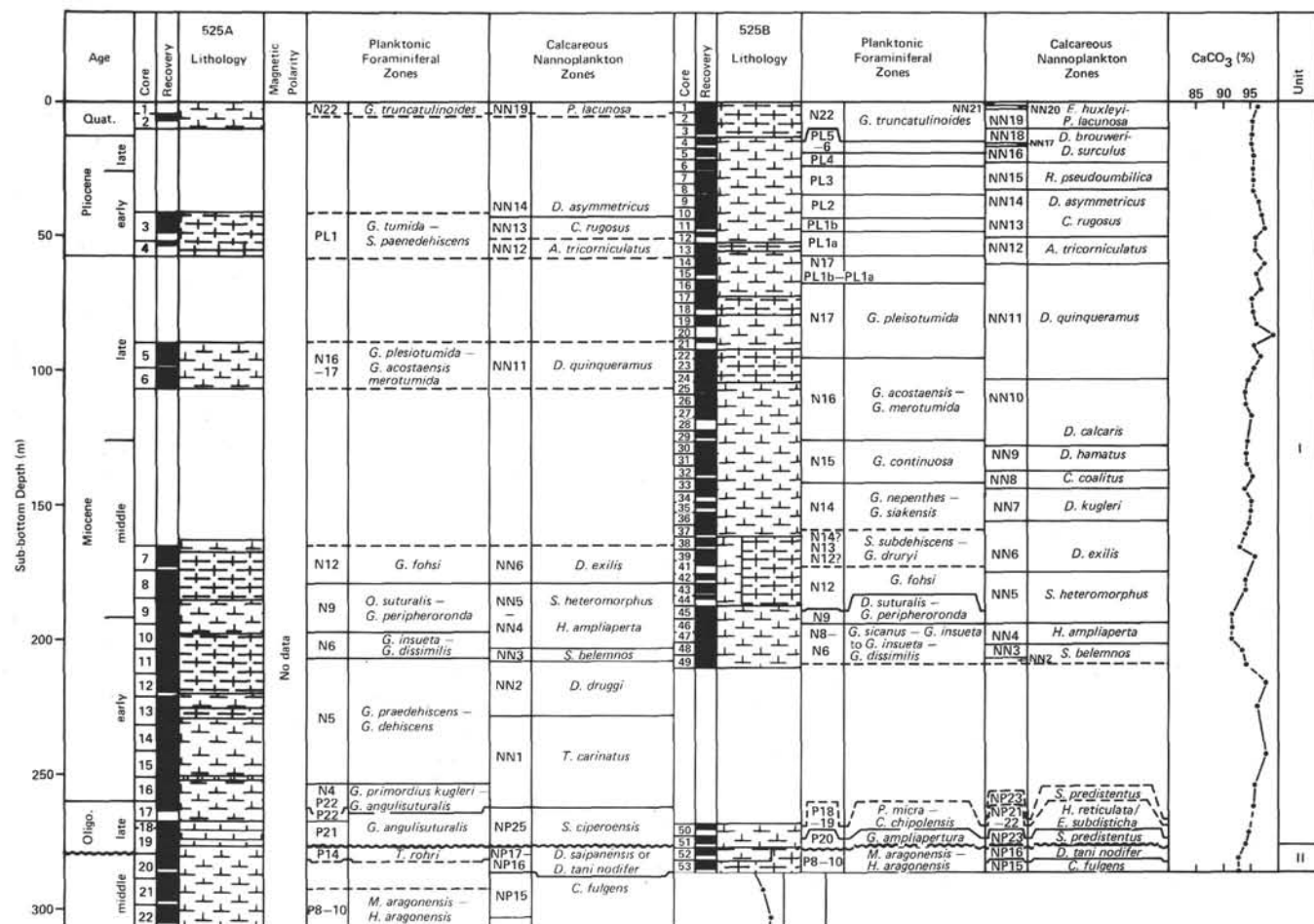Figure 3. Site 526 stratigraphic summary. See Figure 4 for key to symbols.
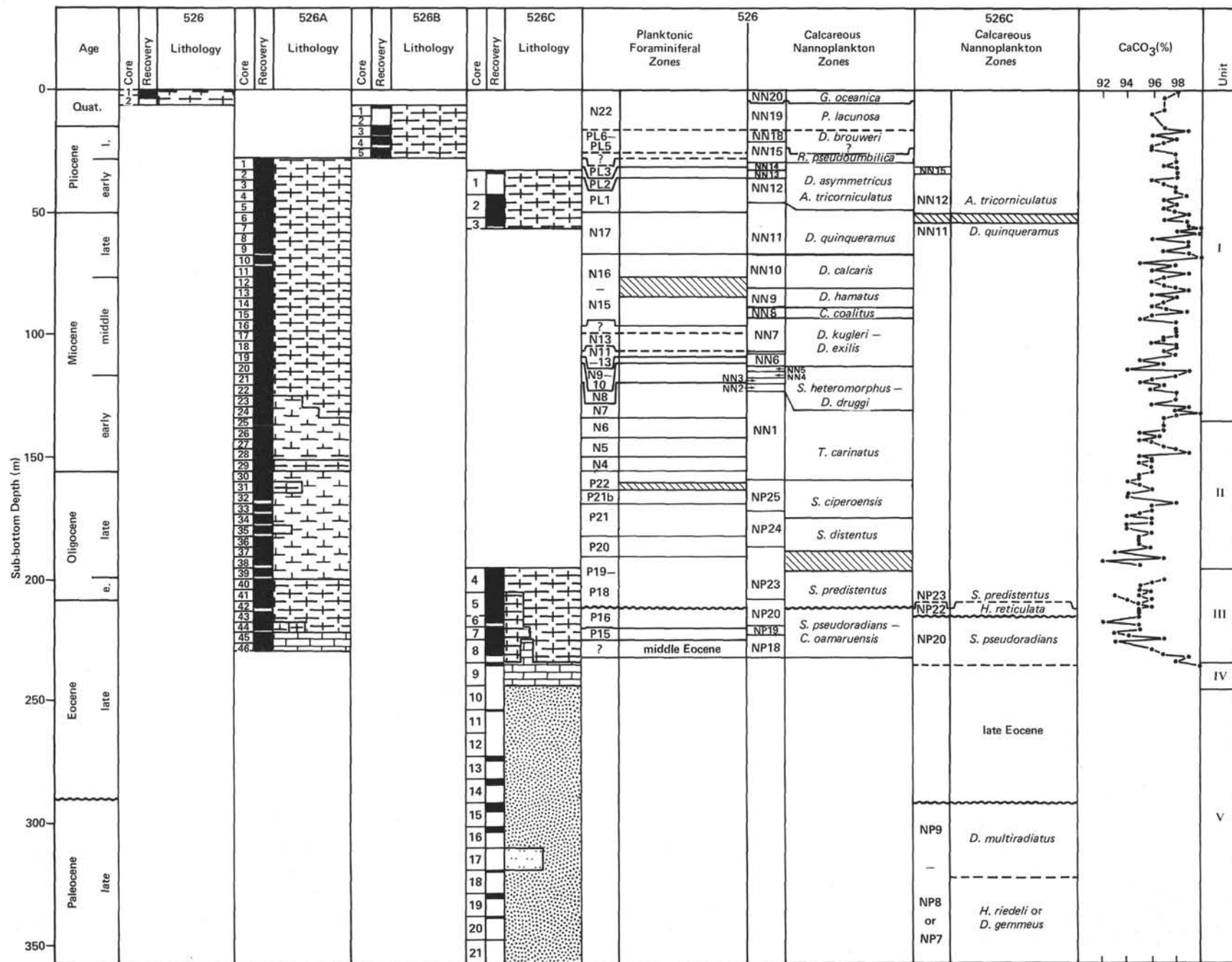
Figure 4. Site 525 stratigraphic summary. Hole 525 results (3.6 m recovery) are not shown.

ary at 452 m sub-bottom. The oldest sediments belong in the late Campanian. The carbonate content of this unit is generally less than 50%. Beautifully preserved biogenic sedimentary structures are present throughout the section. At the base of Unit III and overlying the basement complex is a 6 m thick, spectacular turbidite sequence. The lithologic rock types from top to bottom in the turbidite are (1) coarse-grained, limestone-cemented conglomerates with volcanogenic intra-clasts, (2) coarse- to fine-grained sandstones, and (3) siltstones and calcareous mudstones.

Unit IV, consists of 0.2 to 2.0 m sections of bioturbated, marly limestones and volcanogenic sediments interlayered within the basalt in the acoustic basement, here called the basement complex.

We drilled 103 m into this basement complex. The upper ~ 20 m is a green gray, highly altered, vesicular, aphyric basalt. The remainder of the basalts are gray to black, moderately altered, vesicular, predominantly aphyric flows and pillows with glassy margins and numerous calcite veins. Most of the large vesicles are filled with calcite and minor amounts of pyrite. The groundmass has a subophitic texture consisting of intergrown plagioclase and clinopyroxene. The biostratigraphy and shipboard paleomagnetic results are consistent with crustal formation at time of Magnetic Anomaly 32 (e.g., Campanian).

Site 529, on crust of Magnetic Anomaly 31–32 age (mid-Maestrichtian–late Campanian), is located near the upper part of the slope on the Walvis Ridge transect; its primary objective was to sample complete, well-pre-

served sections missed at the other sites. The site was continuously cored to a sub-bottom depth of 417.0 m. The recovery rate was 74%.

Three major sedimentary lithologic units (Fig. 5) are observed:

Unit I, extends from the mud line to 160 m sub-bottom (lower Oligocene) and consists of a very homogeneous white to pinkish gray foraminiferal–nannofossil ooze. Carbonate content is 95%. There is a hiatus from lower Pliocene to middle Miocene and most probably within the middle Miocene. Slump structures occur in the lower Pleistocene, the upper part of the lower Miocene, and the middle Oligocene.

Unit II, extends from 160 to about 284 m sub-bottom (upper Paleocene) and consists of pink nannofossil ooze and chalk with relative amounts of chalk increasing with depth. Carbonate content is near 90%. There are minor chert layers in the bottom half of the unit.

Unit III, extends from 284 to 417 m (bottom of hole—upper Maestrichtian) and consists of light to olive gray foraminiferal–nannofossil chalks. Preservation of biogenic sedimentary structures is excellent. Carbonate content is nearly 85%. Chert layers occur in the upper half of the unit. A large-scale slump deposit is present in the upper Paleocene, and there are other small-scale slumps, one of which is just above the Cretaceous/Tertiary boundary. Volcaniclastic sediments are abundant in the lower part of the unit. The basement complex was not reached.

Site 528, on crust of an age between Magnetic Anomalies 31 and 32 (mid-Maestrichtian to late Campanian) is located midway up the western flank of the Walvis Ridge transect. Two holes give a complete section from the seafloor to the top of a basement complex at 474 m
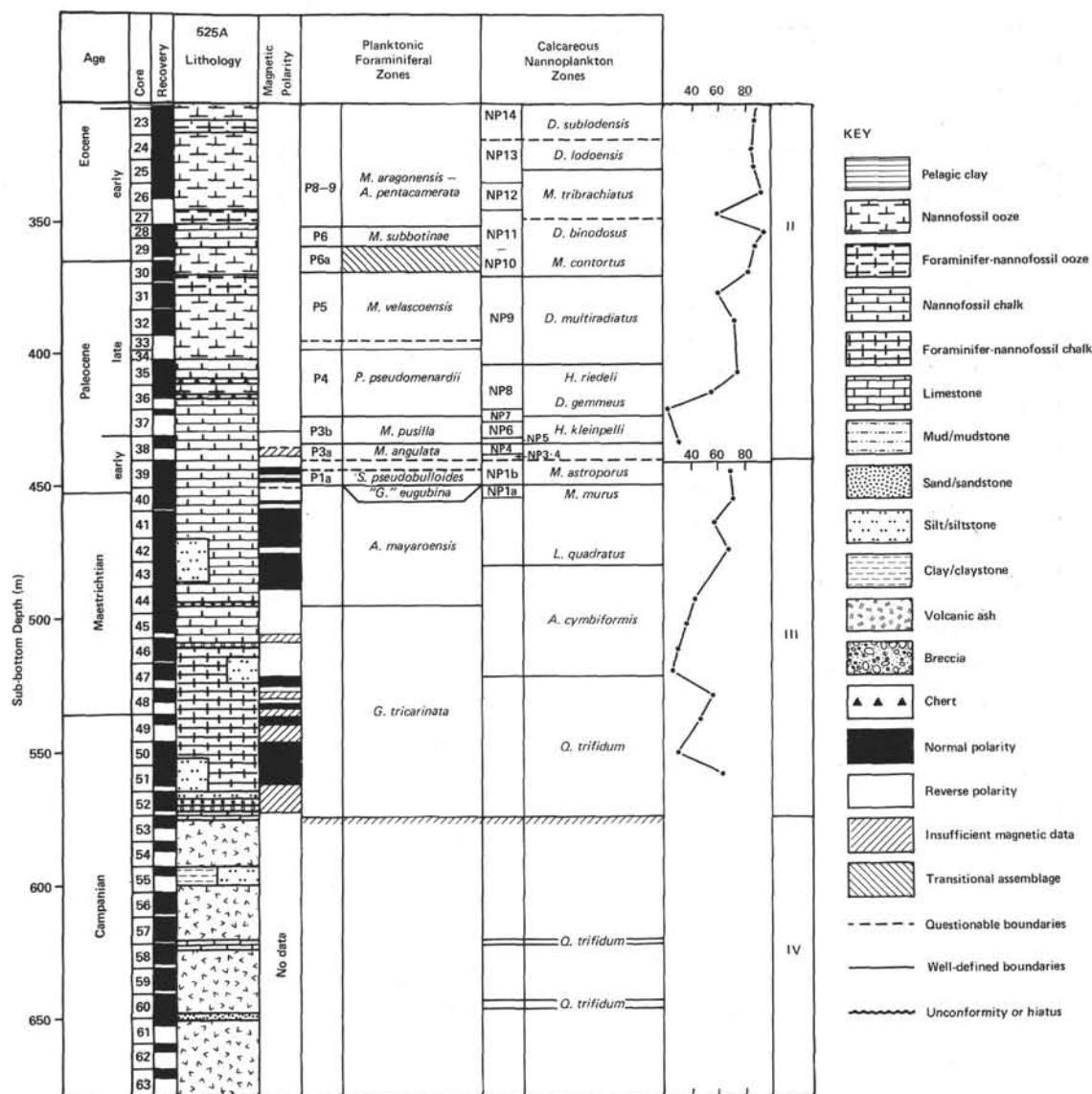
Figure 4. (Continued).

sub-bottom. An additional 80 m were drilled into the basement complex. A good sonic velocity log was obtained in the basement hole.

Four sedimentary lithologic units (Fig. 6) are present:

Unit I, from the seafloor to about 160 m sub-bottom (lower Miocene–upper Oligocene), consists of dominantly white nannofossil and foraminiferal-nannofossil oozes. Calcium carbonate is 90%.

Unit II, from ~160 to 383 m sub-bottom (lower Paleocene), consists of pinkish gray nannofossil oozes and chalks with chalks increasing at depth. Chert fragments occur in the lower half of the unit. Calcium carbonate content is 85 to 90%.

Unit III, from 383 m sub-bottom (lower Paleocene, near the Cretaceous/Tertiary boundary) to the basement complex at 474 m sub-bottom, consists of alternating sedimentary patterns of light gray to reddish brown nannofossil chalks and greenish gray volcanogenic sandstones and mudstones. Turbidites are present near the base of the unit. Carbonate content varies from 30 to 90%.

Unit IV, consists of approximately 0.5 to 5.0 m sections of nannofossil chalks, calcareous mudstone, and volcanogenic sediments interbedded within the basement complex. The oldest nannofossils obtained in the sediments both above and within the basement complex are from the *Arkhangelskiella cymbiformis* Zone (Maestrichtian).

We drilled 80 m into the basement complex. Seven cooling units, ranging in thickness from 3 to 17 m, were defined, each separated by sediment as described above in Unit IV. The seven units are of two basic types. The first is a fine- to medium-grained, slightly to moderately altered, highly plagioclase, phyric basalt with sparse clinopyroxene and olivine phenocrysts. The second is finegrained, moderately altered, vesicular, aphyric to sparsely plagioclase, phyric basalt flows. Both types have subophitic textures.

The biostratigraphy and shipboard paleomagnetic results (Fig. 6) are consistent with crustal formation between the times of Magnetic Anomalies 31 and 32 (middle Maestrichtian–late Campanian).

Site 527, on crust of Magnetic Anomaly 31 age, is the deepest site drilled on the western flank of the Walvis Ridge transect. One rotary-drilled hole provided a complete sedimentary section from the seafloor to the top of a basement complex at 341 m sub-bottom. An addition-
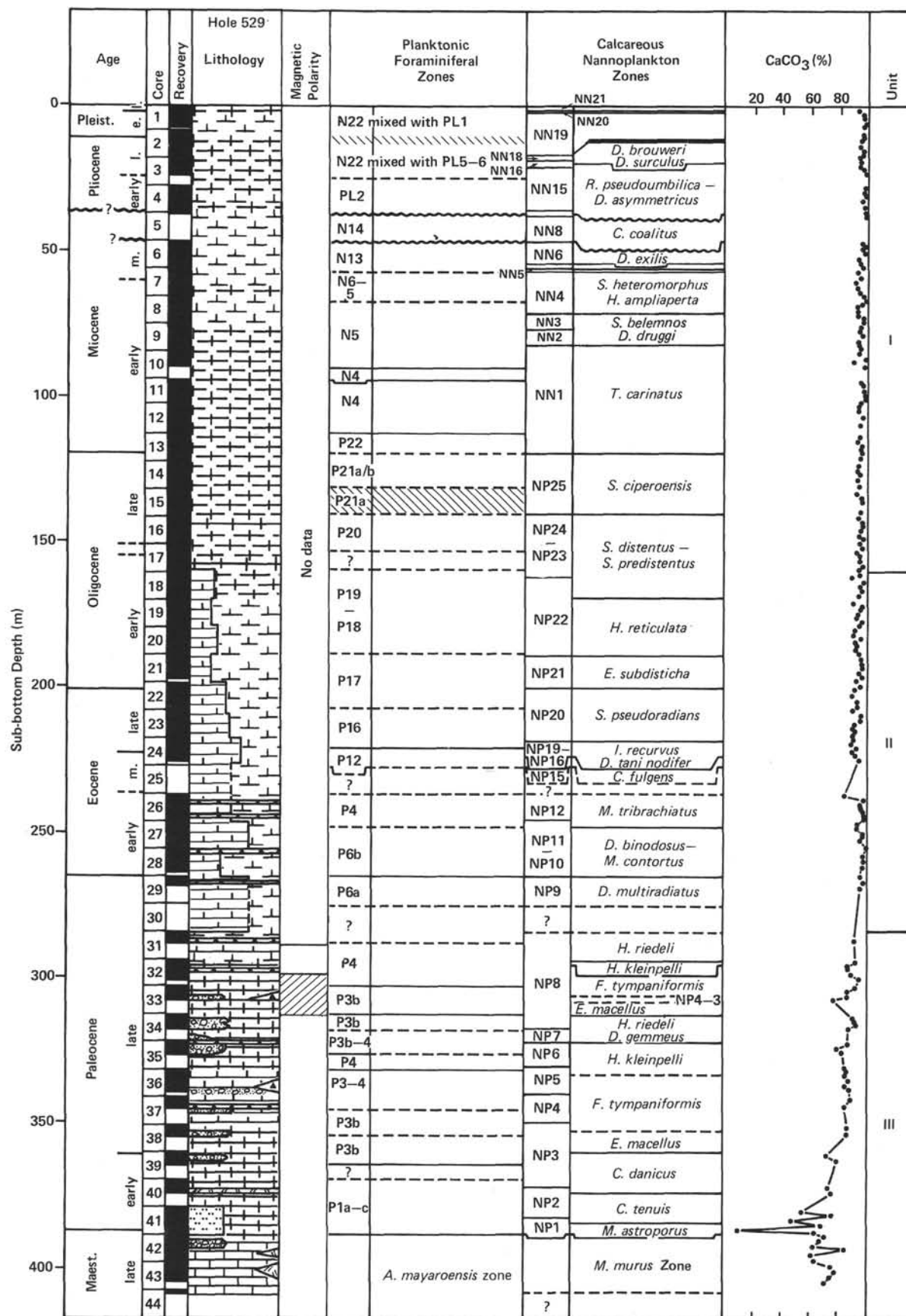
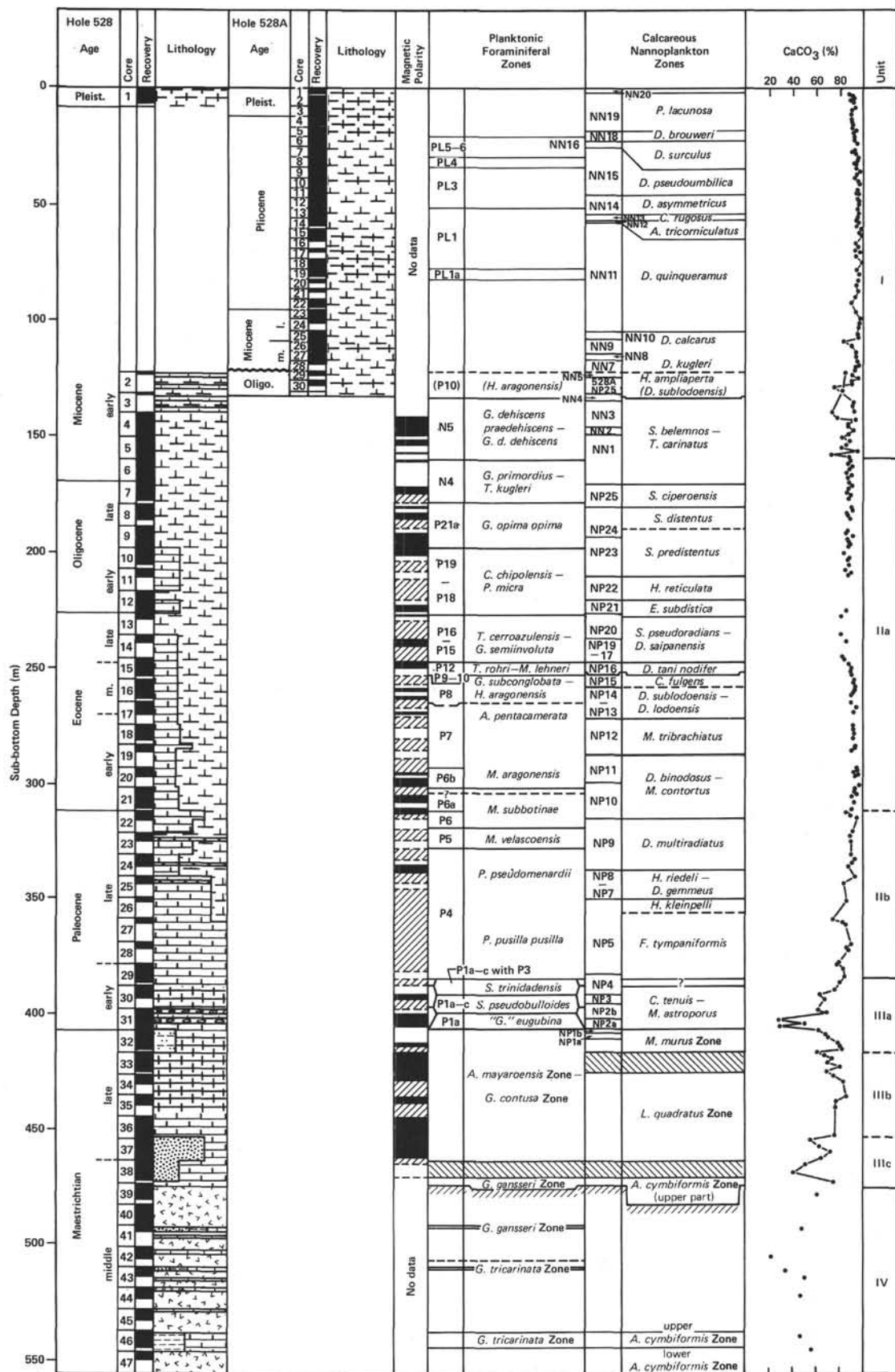Figure 5. Site 529 stratigraphic summary. See Figure 4 for key to symbols.

Figure 6. Site 528 stratigraphic summary. See Figure 4 for key to symbols.

al 44 m were drilled in the basement complex. A density log was run before the hole caved in.

Five major sedimentary units were observed (Fig. 7):

Unit I, from 0 to 102 m sub-bottom, consists of a very homogeneous white nannofossil and foraminiferal–nannofossil ooze of Pleistocene to late Miocene age. The carbonate content is near 95%.

Unit II, from 102 to 142 m sub-bottom, is a brown, marly nannofossil ooze to nannofossil clay (upper Miocene to upper Eocene) with carbonate content ranging from 20 to 95%. Quasi-cyclic patterns in carbonate sedimentation begin in this unit. A major decrease in sedimentation rates or a hiatus is observed between mid-Miocene and lower Oligocene sediments in this unit.

Unit III, from 142 to 275 m sub-bottom, consists of alternating beds of nannofossil chalks and oozes; chalks increase with depth. Carbonate content is near 85%.

Unit IV, extends from near the Cretaceous/Tertiary boundary at about 275 m sub-bottom to the top of the basement complex at 341 m and is a reddish brown, muddy, nannofossil chalk. Noncalcareous components consist mainly of volcanogenic sediments.

Unit V, consists of 0.02, 0.60, and 3.50 m thick sections of nannofossil limestone and carbonate mudstones interbedded within the basaltic basement complex. A very sharp increase in calcium and decrease in magnesium within the pore fluids are observed here. The oldest sediment obtained both above and within the basement complex is mid-late Maestrichtian.

We cored 44 m into the basement complex and were able to define five basalt units separated by sediment interlayers. The upper four are medium-grained plagioclase–olivine–clinopyroxene phyric basalt with large plagioclase and altered olivine phenocrysts. The lower basalt unit is a more altered aphyric basalt. All units are massive flows.

The biostratigraphy and shipboard paleomagnetic results are consistent with crustal formation at the edge of magnetic Anomaly 31 for Site 527.

Although some obvious differences are observed between the shallowest and deepest sites, the sediment lithologies are generally uniform from site to site. From top to bottom, nannofossil and/or foraminiferal–nannofossil oozes grade into ooze and chalk sequences; the ooze/chalk ratio decreases with depth and chalks finally predominate. Volcaniclastic sedimentation increases near basement. Within the basaltic basement complex, interbedded nannofossil chalks, limestones, and volcaniclastic sediments are observed. The carbonate content is high (>90%) throughout most of the lithologic columns but tends to drop near the bases of the columns. In addition, biogenic and primary sedimentary structures are generally poorly preserved to absent near the tops of the columns but tend to be preserved deeper in the sections. In particular, graded turbidite sediments are found near the bottoms of the columns. All of the basement sites have basalt flows with intercalated sediment. The basalts range from aphyric to plagioclase–olivine–clinopyroxene phyric.

Paleomagnetic Results

The results of the paleomagnetic measurements are included in Figures 4–8. The white, unlithified oozes of Pliocene to mid-Miocene age at all sites proved to be too weakly magnetized for measurement even with a superconducting rock magnetometer. The remaining Neogene material was contaminated by a strong viscous remanence, acquired during sample handling, that could not be reli-

ably removed. Thus, detailed study was confined to undisturbed Paleogene rotary-drilled cores, and especially the lithified lower Paleocene to Cretaceous interval at Sites 525, 527, 528, and 529. The latter proved to be quite stably magnetized, with median demagnetizing fields of 200–300 Oe and directional change of less than 20° over a 600 Oe coercive force range. Forty-three pilot samples underwent detailed AC demagnetization in order to determine the optimum field for cleaning treatment of samples. The results show a record that is completely consistent with the paleomagnetic reference section at Gubbio, Italy (Alvarez et al., 1977). The Cretaceous/Tertiary boundary occurs near the top of the reversed interval between Magnetic Anomalies 29 and 30. The complete Paleocene–Cretaceous sequence of Anomalies 28–31 was recognized at all four sites, and Anomalies 25, 26, 27, and 32 are seen at some sites. Figure 8 shows a summary diagram along with the preferred time scale of Ness et al. (1980). The basement ages derived from these magnetic measurements indicate that at Site 525 the basement is of Anomaly 32 age; at 527, Anomaly 31, and at 528, Anomaly 31. These data are consistent with the biostratigraphic ages and mapped crustal anomalies, which suggest that the Walvis Ridge was formed by seafloor spreading processes at a mid-ocean ridge.

IGNEOUS PETROLOGY

Aphyric basalts occur at all three sites at which basement was penetrated, but moderately to highly phyric varieties are restricted to the two flank sites. Significant compositional differences exist between these two types. Representative major-element analyses (Richardson et al., this volume; Table 2) illustrate some features of a probable overall compositional trend from the ridge crest down into the adjacent ocean basin. The sample from the ridge crest Site 525 is an aphyric basalt from a glassy pillow margin. It has the chemistry of a mildly quartz-normative tholeiite with high K_2O, TiO_2, P_2O_5 and Fe_2O_3 contents similar to those encountered in more evolved examples of mid-ocean ridge basalt (MORB) from East Pacific spreading centers (Clague and Bunch, 1976). The sample from the deepest Site 527 is a highly plagioclase phyric basalt from a flow interior. Its chemistry is that of a mildly olivine-normative tholeiite with K_2O, TiO_2, and P_2O_5 contents similar to those in typical MORB, although higher FeO and lower MgO indicate a somewhat more evolved magma.

The major element chemistry of basalts from the Walvis Ridge crest resembles neither that of typical MORB previously recovered from the South Atlantic (Frey et al., 1974) nor that of alkalic basalts on the spatially associated island of Tristan da Cunha (Baker et al., 1964). In addition, the ridge crest basalt trace-element and Nd–Sr–Pb isotopic characteristics (Richardson et al., 1982) are unparalleled among ocean-floor tholeiites. The closest analogs are the tholeiitic basalts of the Ninetyeast Ridge in the Indian Ocean (Hekinian, 1974), which have similar Sr isotopic characteristics (Whitford and Duncan, 1978). The incompatible trace-element and isotopic systematics of the Walvis Ridge basalts suggest derivation by partial melting of mantle which had become het-
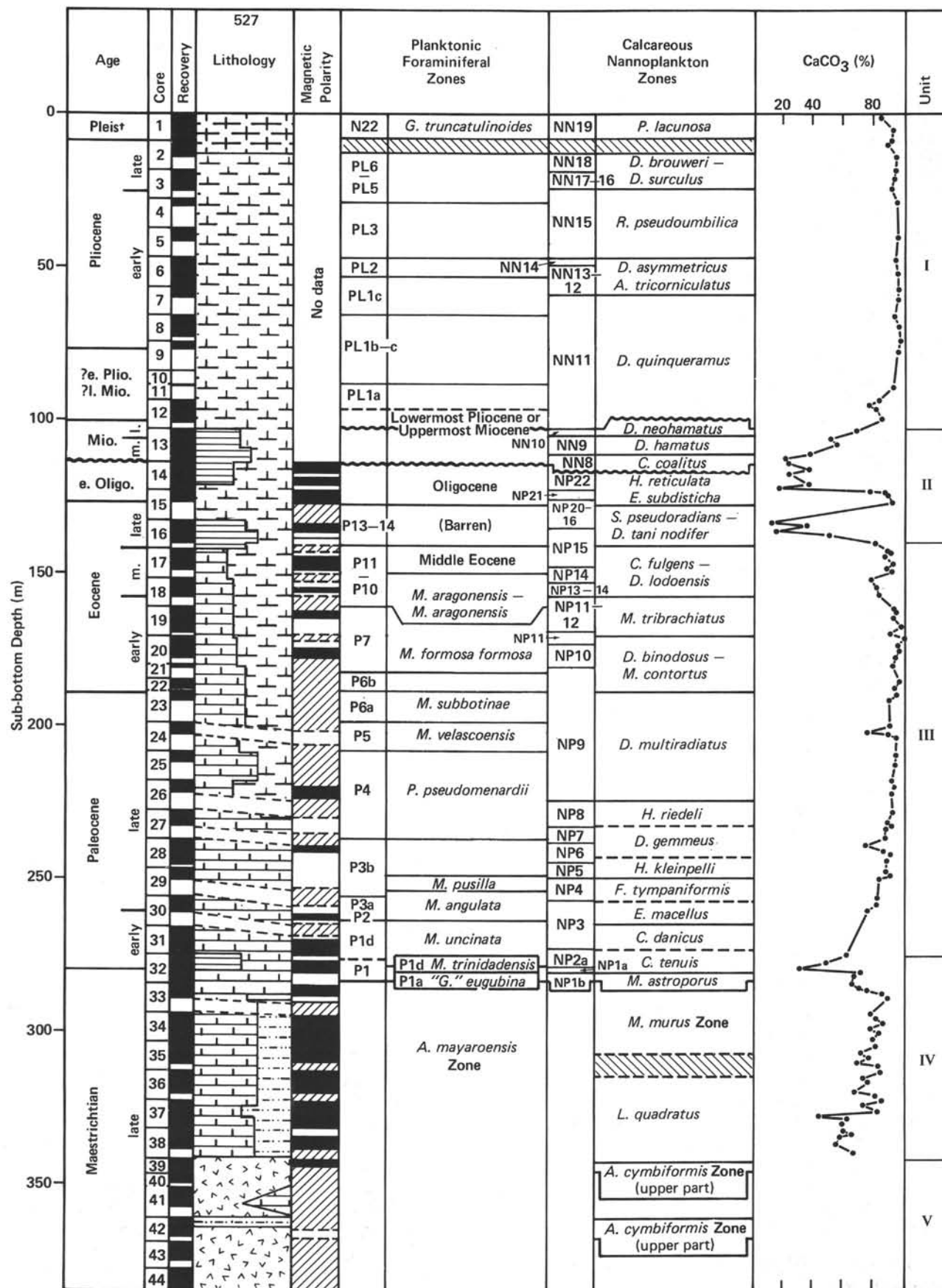
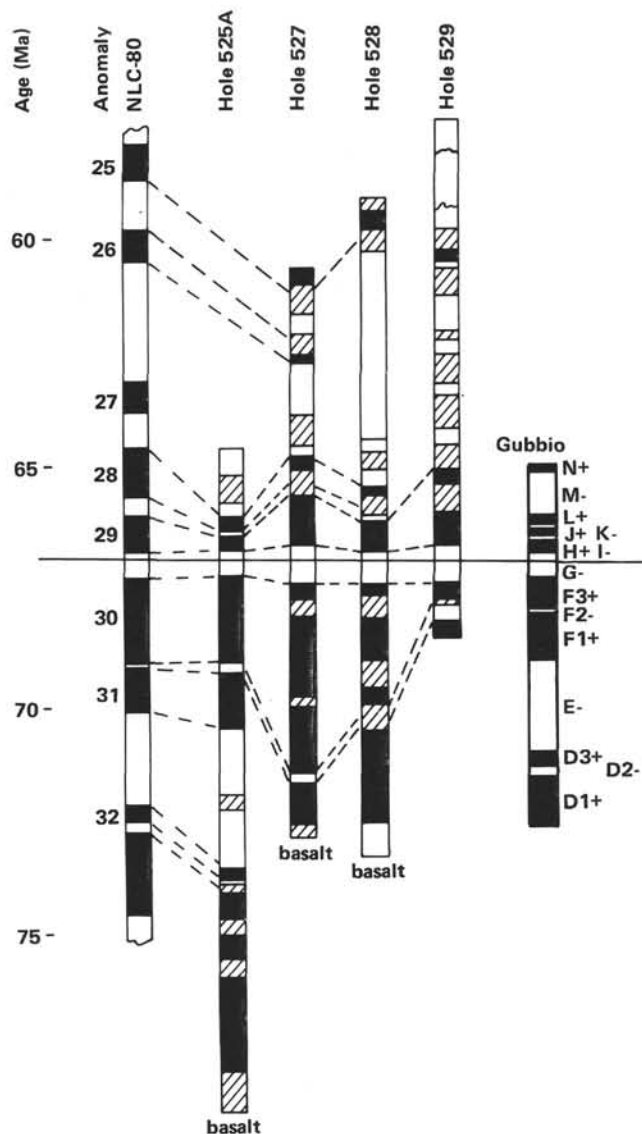Figure 7. Site 527 stratigraphic summary. See Figure 4 for key to symbols.

Figure 8. Summary diagram of Late Cretaceous/early Tertiary paleomagnetic results from four Leg 74 sites using the time scale of Ness et al. (1980), with comparisons to the seafloor-spreading anomaly pattern and the paleomagnetic measurements of the Gubbio section (Alvarez et al., 1977). Black intervals indicate normal polarity; white intervals indicate reversed polarity; hatched intervals (Leg 74 sites) are areas of no recovery.

Table 2. Representative average XRF analyses of basalts from the Leg 74 Walvis Ridge transect.

	Sample 525A-59-4, 25 cm	Sample 527-41-4, 10 cm
Depth[a]	61	14
SiO_2	50.20	48.82
TiO_2	2.49	1.17
Al_2O_3	13.95	16.91
Fe_2O_3	12.92	10.79
MnO	0.19	0.17
MgO	5.33	5.86
CaO	9.49	12.66
Na_2O	2.49	2.52
K_2O	1.03	0.17
P_2O_5	0.31	0.10
LOI	0.90	0.19
H_2O^-	0.51	0.93
Total	99.82	100.29

CIPW Norms[b]

Q		2.97	0.00
OR		6.08	1.00
AB		21.05	21.30
An		23.83	34.31
WO		8.84	11.60
EN	DI	4.44	6.16
FS		4.19	5.07
EN	HY	9.05	5.03
FS		8.55	4.14
FO	OL	0.00	2.51
FA		0.00	2.28
MT		2.63	2.20
IL		4.74	2.23
AP		0.72	0.23

[a] Depth below top of basement (m).
[b] Norms computed on basis of

$$\frac{Fe^{2+}}{Fe^{2+} + Fe^{3+}} = 0.86.$$

erogeneous because of the ancient introduction of small-volume melts and metasomatic fluids (Richardson et al., this volume; Thompson and Humphris, this volume). The relatively low compatible trace-element contents of the Walvis Ridge basalts indicate that they further evolved by fractional crystallization prior to eruption (Richardson et al., this volume). If the Walvis Ridge represents a trace of the Tristan da Cunha hot spot (Liu and Schmitt, this volume) then the composition of the erupting magmas has changed with time, suggesting mantle heterogeneity (Thompson and Humphris, this volume).

Biostratigraphy and Evolution of Walvis Ridge Floras and Faunas

Within the Leg 74 area, sedimentation commenced upon the Walvis Ridge in the early Maestrichtian (*Glo-*

borotalia tricarinata foraminiferal zone or *Quadrum trifidum* nannofossil zone). Sediments were deposited between basaltic lava eruptions. Shallow-water faunas containing *Inoceramus* and turbidites from shallow pinnacles are in places abundant. Benthic faunas and the ratio of the planktonic to benthic foraminifers in these sediments agree with the estimated depth of basalt eruption predicted by normal thermal subsidence models (Table 3). The correlation of standard nannofossil zones to magnetic datums was also possible in the Walvis Ridge sites. Nannoplankton and planktonic foraminifers of the Maestrichtian are typical of middle latitudes. Preservation varies among the sites and appears to be strongly affected by the amount of sedimentary overburden. Nannofossils are moderately preserved throughout, but foraminifers are poorly preserved at the shallow Site 525 and intermediate Site 529; the best preserved Paleogene faunas are found at the deepest Site 527.

The Cretaceous/Tertiary boundary interval is included in four continuous sedimentary sequences which contain diverse nannofossil and foraminiferal biotas. Substantial volcanic material was added to the calcareous sediments below the boundary at all sites. Just below the

Table 3. Fossil criteria for paleoenvironmental and paleodepth estimation of basal, Cretaceous sediments at Leg 74 sites.

Site	Age/Zone at Hole Bottom	Paleoenvironment	Fossil Criteria
525	*Globotruncana tricarinata*	Slope	Large lenticulinids *Palnula* sp. Abundant *Inoceramus* *Gavelinella* cf. *velascoensis*
526	late Paleocene	Carbonate platform	Coral & invertebrate sands *Rotalia* sp. *Asterocyclina* sp. Large lenticulinids
527	*Abathomphalus mayaroensis*	Bathyal	*G.* cf. *velascoensis* *Nuttalides truempyi* *Gyroidina* spp. *Inoceramus*
528	*G. tricarinata*	Bathyal	*Gavelinella* cf. *velascoensis* *N. truempyi* Gyroidinids *Inoceramus*
529	*A. mayaroensis*	Bathyal	Gyroidinids *N. truempyi* *Gavelinella* sp.

boundary at Site 525 there is a thin zone of blue gray sediment containing a warmer-water foraminiferal fauna than those in cores below, implying the incursion of slightly warmer surface waters into this area just before the terminal Cretaceous event; however, isotopic data indicate a temperature maximum just above the Cretaceous/Tertiary boundary (Shackleton, Hall, and Boersma, this volume). All sediments are calcareous oozes with moderately well preserved nannofossils, but not particularly well preserved foraminifers.

The basal Tertiary *G. eugubina* Zone was recovered, attesting to the relative completeness of the sedimentary section. Paleocene faunas are typical of middle latitudes, and floras contain temperate water mass indicators. The shallowest Site 526 probably was close to sea level at this time and contained a carbonate shelf fauna. Sedimentation through the Paleocene appears to have been more continuous at the deeper than at the shallower sites, in that several foraminiferal zones are not identified at Sites 525 and 529 near the end of the early Paleocene. However, no significant breaks were found in the nannofossil biostratigraphic sequence of the early Paleocene. Average accumulation rates (Fig. 9; Shackleton et al., this volume) were lower in the early Paleocene than in the late Maestrichtian. Some of the best preserved nannofossils are found in the upper Paleocene of Site 529, despite the large overburden at this site. The Paleocene/Eocene boundary was easily recognized by the disappearance of the benthic foraminifer *Gavelinella beccariformis* and by the first appearance of the calcareous nannofossil *Discoaster diastypus*.

Early Eocene faunas are relatively well preserved at all sites and benthic foraminifers indicate deposition at intermediate water depths. Planktonic faunas contain sufficient warmer-water elements to indicate warmed surface waters in this area. Preservation worsens markedly and the South Atlantic episode of poorly preserved middle Eocene sediments (Boersma, 1977) is evidenced
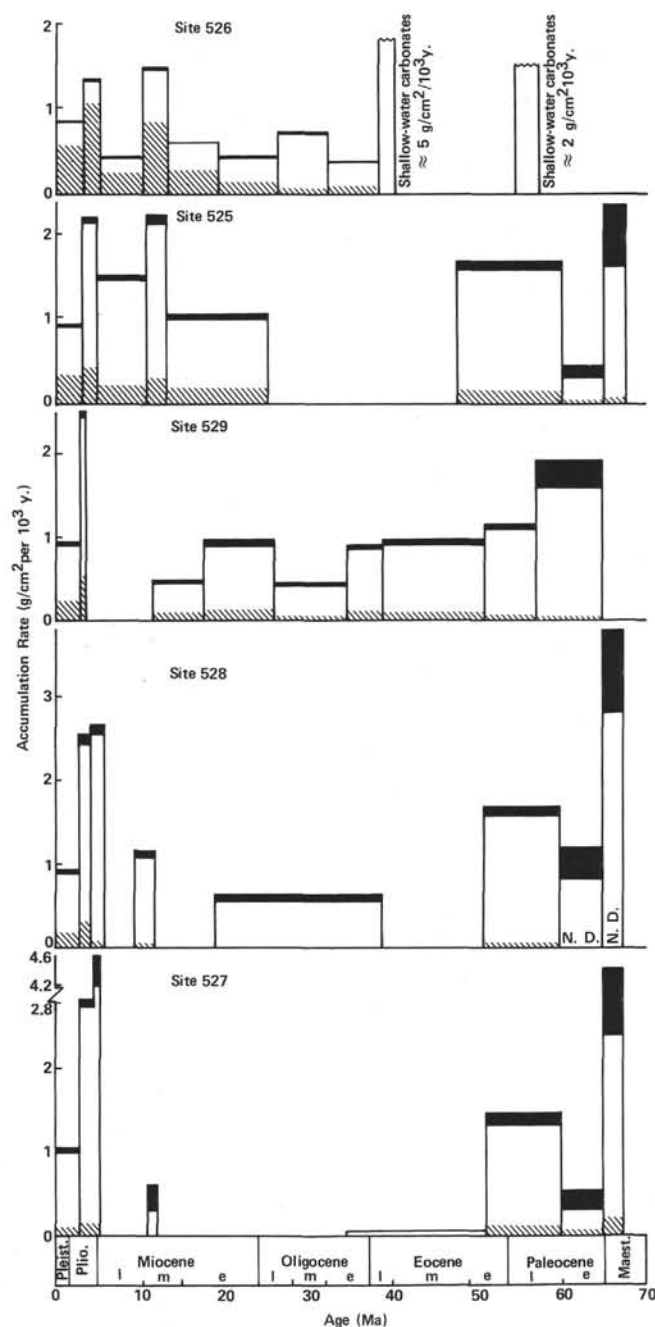

Figure 9. Sediment accumulation rates for the Leg 74 sites, arranged according to water depth from shallow (top) to deep (bottom). Accumulation rates were calculated for three separate components: coarse-grained (> 63 μm) material (dominated by foraminifers and indicated by diagonal shading); fine-grained carbonate (< 63 μm, dominated by calcareous nannoplankton; and noncarbonate sediments (indicated by shading). Accumulation rates for each component were averaged over all intervals recovered. Hiatuses were excluded in the calculation of averages, as were the shallow-water sediments of Site 526 (Fig. 10). "Not determined" indicates lithified intervals where sediments could not be separated into size fractions.

here on the Walvis Ridge. Few well-preserved sequences from the middle into upper Eocene were found at any site. By late Eocene time Site 527 was approaching the paleo-CCD and most of the foraminifers are dissolved. Nevertheless the nannoflora were useful for the zonation in this interval. Little upper Eocene sediment was recovered at any of the other sites. The faunas contain typical middle-latitude species and sediments are nearly all carbonate oozes. At this time the shallowest Site 526 lay near the shelf/slope transition; planktonic oozes contain large amounts of shallower-water sediments and fossils. The preservation of the calcareous nannofossils is poor through the Eocene interval; only large species are present.

The Eocene/Oligocene boundary is well preserved and appears continuous at Site 529, where a long transition zone containing moderately to well-preserved biotas was recovered. According to the calcareous nannofossil study, a very condensed interval containing the Eocene/Oligocene boundary is also present at Site 528. At the shallowest site (526) a regression and consequent sediment removal is indicated at this time.

The Oligocene planktonic biotas recovered at Site 529 included several boreal types but mostly temperate species, which are moderately well preserved. *Chiasmolithus altus*, an Oligocene nannofossil species preferring cooler water masses, was also commonly found only at Site 529. A nearly complete section occurs at the shallower Site 526 which, judging by benthic uvigerinid faunas, must have lain at depths of from 600–1000 m at this time. Shallow-water materials were transported into this area during the middle Oligocene, which is marked by increased sediment erosion and by the presence of bryozoan and molluscan debris and a *Uvigerina semivestita* fauna. This may represent the large eustatic sea-level fall indicated by Vail et al. (1977) at 29 Ma. Other sites apparently lay too deep to demonstrate the effects of the regression. Site 527 lay below the CCD for foraminifers through this time. Only at Site 526 was an interval of abundant *Braarudosphaera* detected within the Oligocene (Zone NP23).

The Oligocene/Miocene boundary was cored at four sites; only Site 527 was below the CCD at this time. The boundary is based primarily on the last occurrence of the calcareous nannofossil species *Sphenolithus ciperoensis*, and the *Turborotalia kugleri/Globigerinoides primordius* concurrent ranges. Foraminifers and nannofossils were moderately well preserved, except in sediments adjacent to hiatuses. Benthic foraminifers indicate that sediments were nearly all from intermediate depths, except at Site 527, which contained red clays with no foraminifers and few nannofossils.

It is difficult to establish a zonation within the upper lower to middle Miocene interval using foraminifers because of the lack of tropical index fossils, although the nannofossils present are generally amenable to a tropical zonation. The buildup of the Antarctic ice sheet coincident with the Zone NN5/NN6 boundary is evidenced by a large influx of keeled globorotaliids and forms of *Globigerinoides* that suggest increased niche differentia-

tion and possibly density stratification at the eastern margin of the South Atlantic gyre.

Carbonate oozes of late Miocene age contain middle-latitude and temperate-water floras and faunas; the sections are relatively complete and preservation is moderate.

Three very well preserved and apparently complete Pliocene sections containing boreal and temperate planktonic fossils were recovered. A marked decrease in boreal species and their replacement by a typical middle-latitude fauna is indicated in all the mid-Pliocene faunas coincident within the extrapolated base of the Gauss Chron. The CCD sank below the deepest site (527) near the base of the Pliocene; thus this site also contains fossils that are sufficiently well preserved for detailed climatic studies. This site is on the northwestern end of the transect (Fig. 1). That it may have lain under a slightly different surface water mass in the Pliocene is demonstrated not only by differing planktonic foraminiferal faunas, but by a different sequence of changes in these faunas through the Pliocene. Although a Pliocene section was recovered at Site 529, active slumping has disturbed the upper Neogene sequence there. The upper Pliocene section accumulated at slower rates and is consistently thin at all sites drilled.

Portions of the early to late Pleistocene contained well-preserved temperate floras and faunas in coarse-grained foraminiferal–nannofossil oozes. Slumping of the Pliocene into the lower Pleistocene was found at Site 529.

History of Sedimentation and Carbonate Dissolution

In an area where pelagic sediments are dominated by biogenic carbonate, the main controls on accumulation rate are productivity (supply) and dissolution. Just as changes in carbonate supply reveal changes in the productivity of the near-surface waters, changes in preservation at the seafloor reveal the chemical gradients and paleoceanography of the deeper waters. The sites on this leg were drilled over a wide depth range in order to investigate the history of carbonate dissolution in more detail than is generally feasible. They were closely spaced in order to minimize the effect of areal variation in productivity, and the pelagic supply to the sites was assumed to be uniform. Changes in the average supply rates should reflect temporal (rather than spatial) changes in the productivity of this region of the South Atlantic. At any given time, differences between the sites in accumulation rates should reflect the effects of near-bottom processes such as dissolution, erosion, and winnowing. There is strong evidence that changes in all these factors occurred.

Near Surface Conditions and Productivity Changes

The shoalest site (526, Fig. 1) is likely to have suffered little or no calcite dissolution and changes in carbonate accumulation rates here (particularly coarse-grained carbonate, not subject to removal by winnowing) should reflect changes in carbonate productivity (Fig. 9). Data from this site indicate a peak in productivity at 5 Ma

that is nearly double the average Neogene rates of 1 gm/ cm^2 per 10^3 y. (Shackleton et al., this volume). There was another maximum in productivity in the middle Miocene (near 13 Ma) of somewhat lesser magnitude. These two maxima, seen in the average for almost all sites (Figs. 9 and 10), are surpassed by a third maximum at 23 Ma seen by Shackleton et al. (their Figs. 3, 7, this volume). Figures 9 and 10 are based on a slightly different timescale from Shackleton et al. (this volume) and do not attempt a uniform 1 Ma time resolution. The Oligocene/Miocene maximum seen in the Shackleton et al. study may result in part from an inaccuracy in the timescale used.

The fact that peaks in accumulation at Site 526 (where little or no dissolution is expected) correspond to peaks at other sites suggests that the marked changes in average accumulation rates correspond to productivity changes. This suggestion is supported by further work of Shackleton et al. (this volume) which shows that changes in the accumulation rate of fish teeth (highly resistant to

dissolution) also follow the accumulation rate changes seen in the carbonate fractions.

The third indication of productivity changes comes from measurements of $\delta^{13}C$ on bulk carbonate (Shackleton and Hall, this volume) which provide a measure of the partitioning of carbon in the global budget and of the isotopic contrast between the surface waters and the deep ocean. The lowering of $\delta^{13}C$ in the bulk carbonate (dominated by calcareous nannofossils) suggests a decrease in the biological fractionation of carbon isotopes between deep and shallow waters and is interpreted as a decrease in primary productivity. This study shows a marked drop in $\delta^{13}C$ values at the Cretaceous/Tertiary boundary. There is substantial and sustained recovery in the Paleocene that nearly matches the maxima in accumulation rates of carbonate and fish teeth, but appears to be in advance of the peak values in accumulation by a few million years. This is in sharp contrast to the simultaneous drop in both accumulation rate and $\delta^{13}C$ at the Cretaceous/Tertiary boundary.

Bulk $\delta^{13}C$ data for the rest of the sections recovered on Leg 74 are more sparse (Shackleton and Hall, this volume); however, they do show broad peaks in the mid-Miocene and early Pliocene which correspond to and are slightly in advance of accumulation rate maxima at these times. Thus, the relationship between accumulation rates and $\delta^{13}C$ maxima during the Cenozoic appears distinctly different from the sharp drop in both $\delta^{13}C$ and accumulation rates which occurred at the Cretaceous/Tertiary boundary. At the boundary, both measures of ocean fertility change simultaneously, as if responding to the same forcing function or catastrophic event which caused the extinction of many of the planktonic species. Through the Cenozoic changes in $\delta^{13}C$ precede accumulation rate changes. Many of the Cenozoic changes in accumulation rate and $\delta^{13}C$ are of nearly the same magnitude as noted at the Cretaceous/Tertiary boundary, yet there are no mass extinctions of the plankton, and the accumulation rate maxima appear to occur at the same time as the rapid decline in $\delta^{13}C$ values. This may indicate that the peaks in productivity coincide with the restoration of a more moderate vertical partitioning of the carbon isotopes and that the strong shallow to deep gradients in the carbon isotopes represent a potential for high productivity which is only fully realized at the time such gradients collapse.

Although the data are fewer than those provided for bulk $\delta^{13}C$, the La/Ce ratios for Hole 525A also show large changes (Liu and Schmitt, this volume), particularly in the basal part of the section, that are similar to changes in bulk $\delta^{13}C$ (Fig. 11). The low values in La/Ce are interpreted as indicating either "anoxic" bottom waters or reducing conditions within the sediment. Considering the similarity to the bulk $\delta^{13}C$ changes and the lack of any benthic faunal evidence for anoxia, it seems likely that deep waters of the Late Cretaceous and late Paleocene may have been low in oxygen (high in recycled nutrients) and that pore waters of the rapidly accumulating sediments were further depleted in oxygen.

Using the accumulation rate data as a guide to the productivity history of the southeastern Atlantic, we deduce that in the latest Cretaceous, when the Walvis Ridge
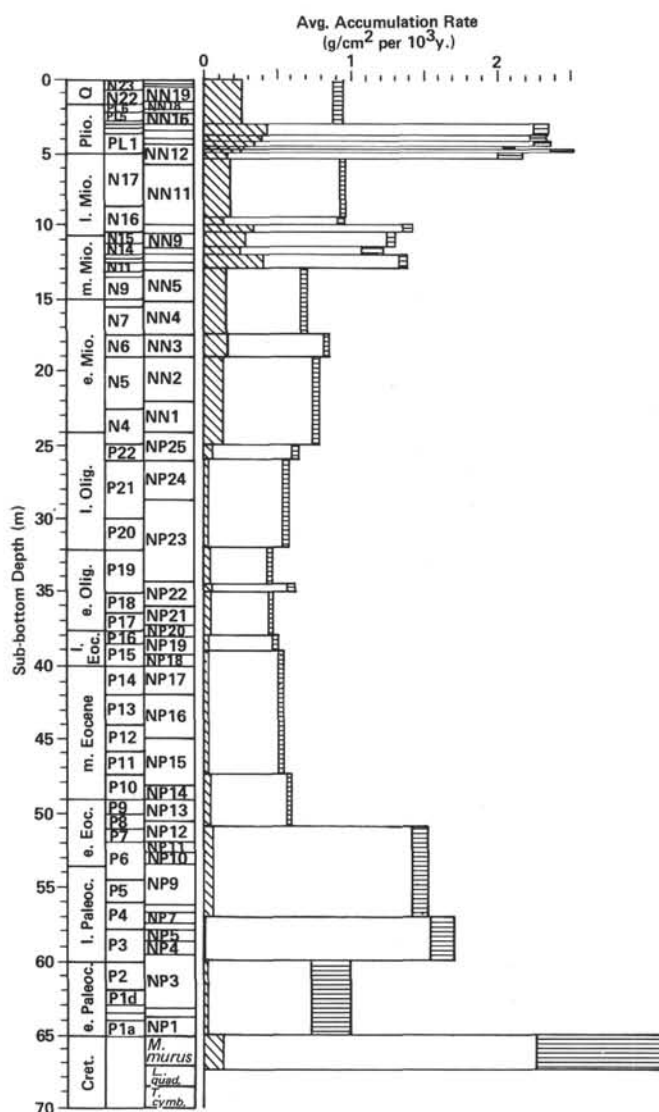

Figure 10. Average sediment accumulation rates for Leg 74 sites. Shading and notation as in Figure 9.
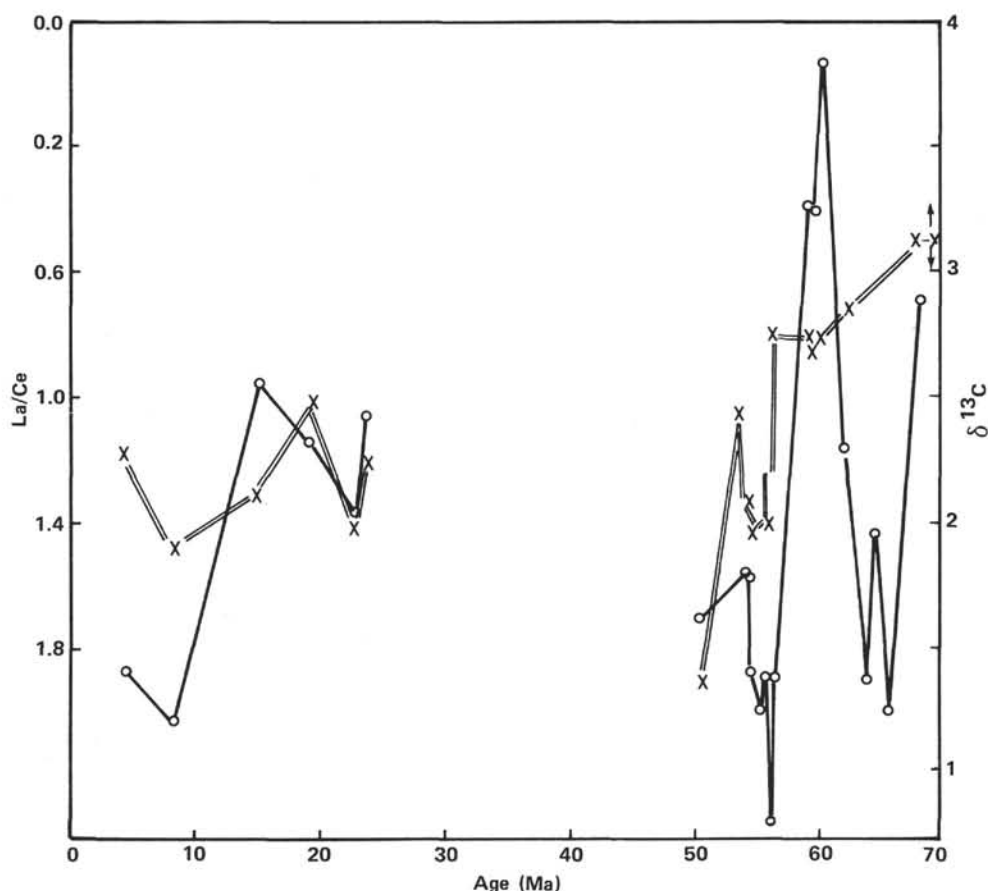
Figure 11. La/Ce ratio (×) versus age at Hole 525A (data from Liu and Schmitt, this volume) compared with bulk $\delta^{13}C$ (○) from the same site (timescale and selected $\delta^{13}C$ data from Shackleton and Hall, this volume).

existed as an archipelago, productivity was about twice what it is today. The drastic drop in productivity at the end of the Cretaceous was followed by a recovery that boosted carbonate accumulation rates to a maximum of 1.5 times modern rates and lasted much of the late Paleocene and early Eocene. The peak accumulation near the Oligocene/Miocene boundary may not have been so large as indicated by Shackleton et al. (this volume), but the final two maxima in the Neogene appear well established. They occurred in the late middle Miocene (1.5 times modern rates) and early Pliocene (twice modern rates).

The high productivity of the Late Cretaceous and early Cenozoic may be associated with intensified surface circulation in a restricted South Atlantic cut by emergent portions of the Walvis and Rio Grande ridges. Sea surface paleotemperatures measured in the late Maestrichtian samples from Leg 74 range between 13 and 16°C (Shackleton, Hall, and Boersma, this volume). On the western side of the Atlantic at this time, temperatures are estimated to have ranged between 18 and 25°C (Willliams et al., in press). This relatively steep zonal temperature gradient of 5 to 9°C (compare the ~2 to 3°C gradient in the modern ocean) suggest a rather strong gyral circulation carrying cooler, subpolar waters northward on the eastern (Walvis Ridge) side and warmer tropical waters southward on the western (Rio Grande Ridge) side.

The marked decrease in productivity at the Cretaceous/Tertiary boundary is noted on both sides of the South Atlantic (Williams et al., in press; Shackleton, Hall, and Boersma, this volume) and is associated with a large turnover in the planktonic flora and fauna. However, there was no large change in the benthic fauna or benthic oxygen isotopes across this boundary. The Cretaceous/Tertiary "catastrophe" was one primarily of the surface waters (Boersma, in press).

If the accumulation rates alone were a true measure of the proportions of this catastrophe, then the sudden drop at the end of the middle Miocene and in the mid-Pliocene might indicate events of nearly equal proportions—at least regionally. Other indicators of near-surface conditions, however, do not point to great changes at these times. The planktonic foraminifers indicate some cooling after a warm mid-Eocene (Boersma; Shackleton, Boersma and Hall; both this volume), a temperate fauna through the Oligocene, and the return of somewhat warmer conditions in the uppermost Oligocene with the introduction of some subtropical forms (Boersma, this volume). The Miocene sections contain faunas that are not well preserved, but by mid-Pliocene times, preservation has improved and boreal elements have been replaced by temperate and even subtropical forms.

This general trend in surface temperature change is given quantitatively by oxygen isotope measurements made on planktonic foraminifers (Shackleton, Hall,

and Boersma, this volume). They follow the Paleogene trend in benthic isotope measurements and show a temperature maximum in the early Eocene, a cooling in the early middle Eocene, and a very rapid and intense cooling at the Eocene/Oligocene boundary that may have been associated with a brief period of Antarctic glaciation (Shackleton, Hall and Boersma, this volume). A rather cool Oligocene is followed by a warming in mid-Miocene time. As in most deep sea isotope records, the planktonic and benthic records tend to diverge in the mid-Miocene with surface waters of the area warming by about 6°C and deep waters cooling slightly as the South Atlantic became thermally isolated from Antarctic waters (Shackleton, Hall, and Boersma, this volume). The oxygen isotope record of the planktonic foraminifers agree with the foraminiferal assemblage studies (Boersma, this volume) and appear to reflect the general history of global cooling and warming rather than a strictly regional pattern of change, limited only to the South Atlantic.

Deep-Water Conditions and Carbonate Dissolution

The Leg 74 sites were planned to provide a "dipstick" in the oceans—located to monitor changes in the dissolution rate and variation in erosion as a function of time and depth. A submarine edifice such as the Walvis Ridge collects sediments that monitor changes in ocean chemistry; however, it also forms a major obstacle to the flow of deep and intermediate waters. As a result, an enclosed deep sea basin may be shielded from certain deep water masses (as the Angola Basin is today), and flow of these waters around and over such an obstacle is intensified. Sediments deposited on such a topographic high can be highly winnowed. Shackleton et al. (this volume) have calculated the accumulation rates of the >63 μm fraction (foraminifer-dominated) fraction separately from the <63 μm fraction (nannofossil-dominated). By separating the coarse and fine-grained accumulation, they have been able to investigate the effects of winnowing, which removes fine-grained material from topographic highs and deposits them on the flanks and in the basins, and to distinguish the effects of dissolution, which usually increase with depth.

Heath et al. (1977) showed a plot of carbonate accumulation rate versus depth and time for Cenozoic deposition in the equatorial Pacific. At any given time, changes in accumulation versus depth were interpreted as a simple, linear, dissolution gradient. Winnowing did not appear to be a problem in the equatorial Pacific; however, on a large aseismic ridge winnowing is a major factor in the deposition of fine-grained carbonate (Shackleton et al., this volume; Moore et al., 1973). Furthermore, if carbonate dissolution is greatly affected by kinetics (Thunell et al., 1981; Morse and Berner, 1972), the intensification of currents around such a ridge may also affect dissolution rates.

The accumulation rate data for the <63 μm and >63 μm actions from Walvis Ridge sites (Shackleton et al., this volume) are shown in Figure 12. In these plots the rate for each million-year increment was plotted at the estimated paleodepth for each site at the time of

deposition (a simple thermal cooling curve was used to estimate paleodepths). The plotted values were then contoured.

The pattern revealed by these time–depth plots is complex. The <63 μm fraction is the most abundant and data on this fraction are more evenly distributed. The first aspect of this plot (Fig. 12A) which is readily discerned is the effect of high rates of supply. The high accumulation rates in the uppermost Cretaceous, the upper Paleocene–lower Eocene, the mid-Miocene and the lower Pliocene are seen as rather broad maxima. The 23–24 Ma maximum shows as a distinct spike, followed by a broad minimum extending to 18 Ma. Another maximum of lesser magnitude is seen in the deeper sites only (527, 528, 529) just above the Eocene/Oligocene boundary.

The second major effect noted in Figure 12A is that of dissolution. In the Upper Cretaceous and lower Paleogene, dissolution at the deeper sites was low. There was a marked increase in dissolution at 46 Ma (mid-Eocene) followed by a drop in the calcite compensation depth (CCD) near the top of the Eocene. The CCD shoaled through the Oligocene and lower Miocene, then deepened, first in the mid-Miocene and again in the upper Miocene through lower Pliocene. The pattern followed in the Cenozoic is more detailed but not greatly different from that given by Berger and von Rad (1972) for the South Atlantic. The present, very deep CCD in the Angola Basin (Ellis and Moore, 1972; Thunell, 1982) appears to have been reached by the final (late Miocene–early Pliocene) deepening.

The most enigmatic feature in Figure 12A is the mid-depth minima in carbonate accumulation. Are they (1) the result of local slumps that removed sections from one or two sites, but have no regional significance, or (2) the result of depth-limited current erosion and/or current-enhanced dissolution? In the Paleogene a dissolution–erosion episode occurs at both Sites 529 and 525. It extends in time from the late Paleocene ($\sim$59 Ma) to the late Oligocene ($\sim$26 Ma) and in depth from 2000 to 2600 m. In the mid-Eocene, the mid-depth minimum in accumulation appears to merge with the deeper minimum that is associated with the very shallow CCD.

The beginning of this episode is associated with slumping at both Sites 525 and 529. It is also near the time that the shoalest parts of the ridge in this area sank below sea level. The slumping could be tectonically induced and associated with the time of rapid ridge subsidence. It could also be associated with erosional episodes within the intermediate water masses.

There are other indications of changes in the bottom waters during this interval. The bulk $\delta^{13}C$ ratio drops precipitously at this time (Shackleton and Hall, this volume), indicating a decrease in the isotopic contrast between shallow and deep waters. This is also a time when massive turnover in the benthic fauna (Boersma, in press) indicates marked changes in the deep and intermediate waters. The next major change in the character of the benthic fauna comes near the top of Zone P21 ($\sim$27 Ma) at Site 529 near the time that the mid-depth erosional episode ends in the next shoaler site (525).
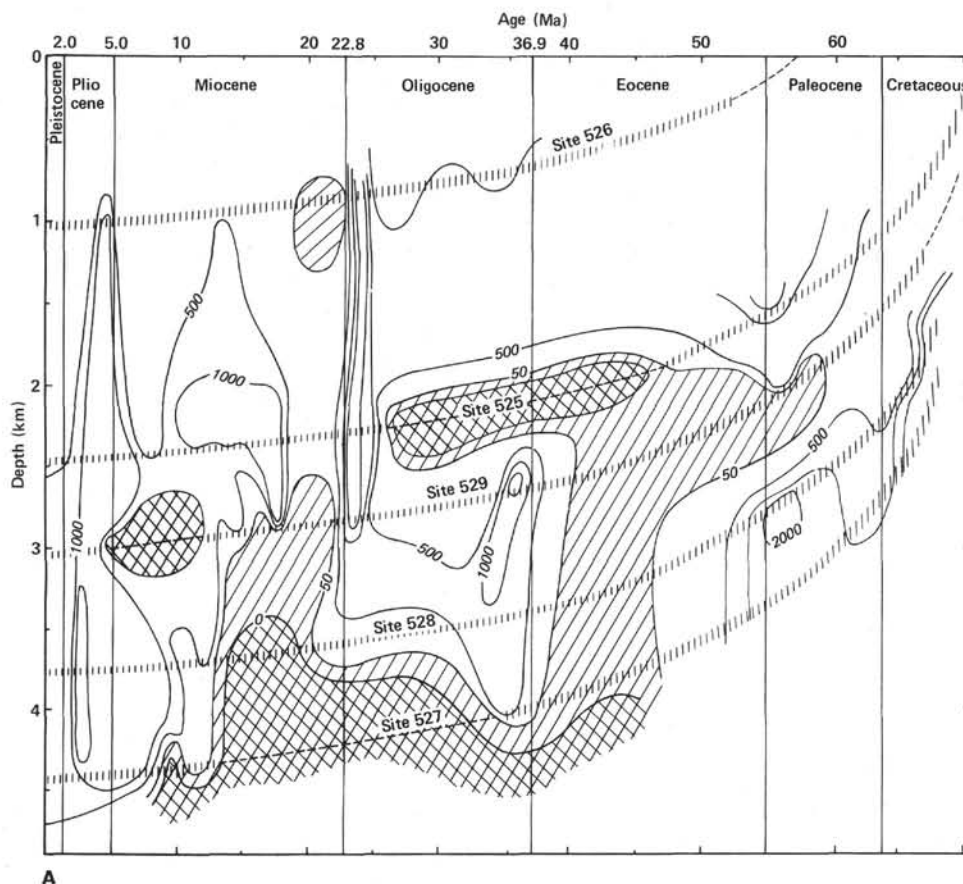
A

Figure 12. A. Carbonate accumulation rate (mg/cm² per 10³ y.) of the ≤ 63 (calcareous nannofossil) size fraction versus age. Data were plotted at 1 Ma increments for each site at the paleodepth of the site. A simple thermal cooling curve was used to estimate paleodepth. The 0, 50, 500, 1000, and 2000 mg/cm² per 10³ y. contours are shown. Regions of no fine-grained carbonate accumulation are shown in dark shading; regions of low carbonate accumulation (≤ 50 mg/cm² per 10³ y.) are shown in light shading. Accumulation rate data are from Shackleton et al. (this volume). B. Carbonate accumulation (mg/cm² per 10³ y.) of the > 63 μm (foraminifers) size fraction. Plotted as in Fig. 12A. Contours are 0, 50, 100, 200, 400, 600, and 800 mg/cm² per 10³ y. Regions with no coarse-grained carbonate accumulation are shown in dark shading.

Thus, it appears that the Paleogene mid-depth minimum in carbonate accumulation is associated with other indicators of change in the deep waters and is likely to represent an episode of erosion and dissolution that is of regional importance. The depth range of Leg 74 sites affected by this episode makes it unlikely that sites located on the flanks of the Mid-Atlantic Ridge and in the basins would be strongly affected. However, the mysterious *Braarudosphaera* chalk of Zone NP23 (Manivit, this volume) may in some way be related to fluctuations in this zone.

A similar mid-depth erosional event is seen at Site 529, extending in time from about 12 to 4 Ma (latest middle Miocene to earliest Pliocene) at a paleodepth of about 3 km. There is a turnover in the benthic fauna at about 13 Ma, where the new late Neogene assemblages first appear (Boersma, in press). This also follows the mid-Miocene drop in the CCD.

The end of the late Miocene erosional event follows the reappearance of the "Oligocene-type" fauna in the benthic foraminiferal population (Boersma, in press) which began in deep sites at about 9 Ma and in shallow

sites at about 5 Ma. The mid-Miocene also marks the beginning of divergence between the planktonic and benthic isotope record (Shackleton, Hall and Boersma, this volume). Thus, there is ample evidence for change in the vertical structure and in the chemical and biological character of the deep ocean during the mid- to late Miocene.

The final feature of Figure 12A noted here is the indication of winnowing effects. At all intervals showing maxima in accumulation rates, the maximum nearly always occurs below the shoalest site. In the Late Cretaceous the maximum is at Site 527, the deepest site drilled. In the late Paleocene, the mid-depth minimum in accumulation rates separates high accumulation rates at deeper and shoaler sites. The early Oligocene maximum is seen only at the deeper sites (2800–4000 m paleodepth). It occurs below the erosional zone of Site 525 and is associated with the deepening of the CCD.

Accumulation rates and dissolution patterns are suspect between 18 and 24 Ma; however, it does not seem possible to change the time scale in a way that totally removes the Oligocene/Miocene maximum in accumu-
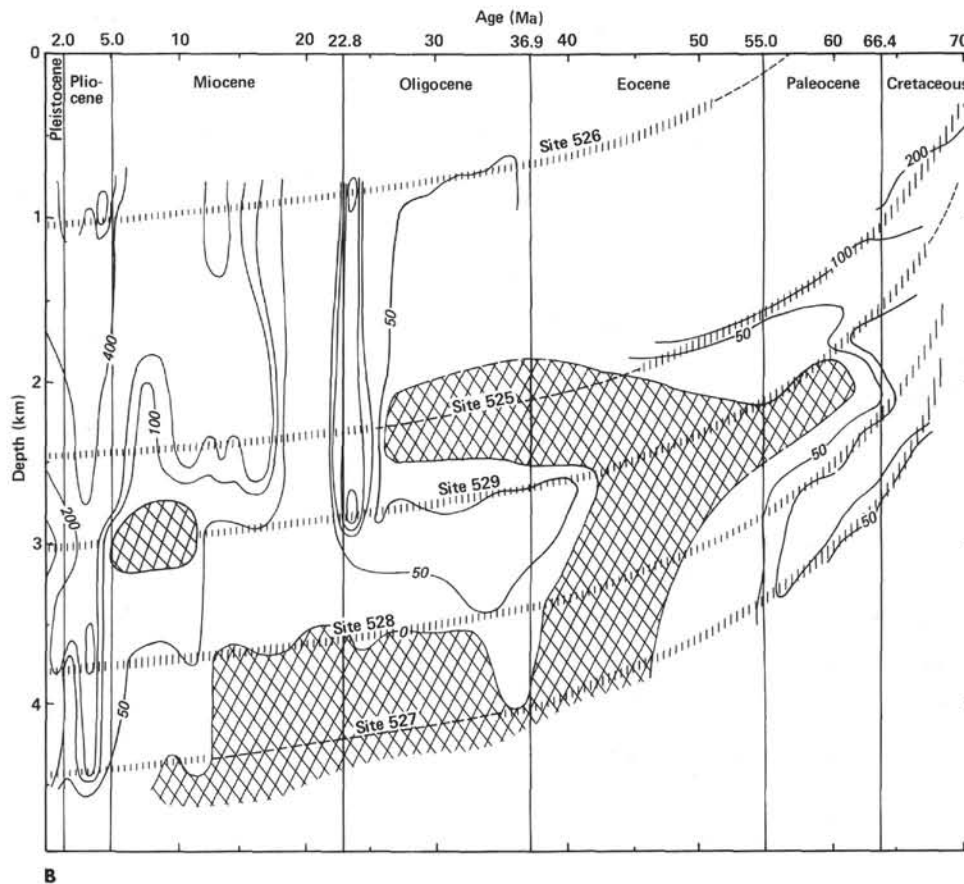
Figure 12. (Continued).

lation. Accumulation rates appear to be only slightly greater at Sites 525 and 529 (2500 to 3000 m paleodepth) than at the shoalest sites (526, 800 m paleodepth).

In the mid-Miocene, after the CCD had shoaled markedly, maximum accumulation rates are found to be at slightly shallower depths (~2400 m). As the CCD falls in the late Neogene, the region of maximum accumulation of the fine-grained carbonate chaff falls with it. In the early Pliocene the maximum is found near 3800 to 4400 m paleodepth.

Although the data are more sparse, the same general features of accumulation and dissolution seen in Figure 12A are also found in Figure 12B, the plot of foraminiferal carbonate (>63 μm) accumulation rates. However, two important additional features are apparent. First, the comparison of rates of accumulation at any given depth indicates that the rates are generally higher in the Neogene than in the Paleogene. Aside from the very high rates in the interval from 23–24 Ma, the rates of the mid-Miocene and younger are three to ten times higher than those of the rest of the Cenozoic. The highest rates of all are found in early Pliocene and younger sediments. These results suggest an evolutionary effect on the supply of foraminiferal carbonates that was first noted by Bramlette (1958). The foraminifers appear to have become quantitatively more important after their mid-Miocene evolutionary bloom and then to have increased their average productivity again during the early Pliocene maximum.

The second point to be made from Figure 12B is the dissolution effect noted by Shackleton et al. (this volume). There is a clear decrease in accumulation rates between Site 526 (800–100 m paleodepth) and 525 (2300–2500 m paleodepth). This indicates significant carbonate loss in the coarse fraction at depths that are comparable to ridge crest depths in most ocean basins, and suggests that dissolution of carbonate can occur at very shallow depths, at least in areas of strong topographic relief.

In summary, there appear to have been several major changes in the deep waters of the Angola Basin. The first recorded by Leg 74 data occurred near the Paleocene/Eocene boundary. There was a major change in the benthic fauna and what appears to have been a mid-depth erosional episode began. Erosion and dissolution was most severe in the middle to upper Eocene, with effects being seen at all sites below 2000 m water depth. The end of this dissolution maximum is at 40 Ma at Site 529 (2600 m paleodepth) and somewhat later, at 37 Ma, in the deepest site (527, at 4000 m paleodepth). The Eocene/Oligocene boundary may be associated with a brief interval of Antarctic glaciation which provided a new source of well-oxygenated water to the South Atlantic.

The mid-depth erosional event continued into the Oligocene and then ended near the time of the second major change in the benthic fauna. Through the Oligocene and into the mid-Miocene the CCD gradually shoaled and then dropped abruptly just following the time of

major glaciation of Antarctica in the middle Miocene and then again in the late Miocene, near 8–9 Ma. A second mid-depth erosional event evidenced at Site 529 may be of only local importance or may be associated with changes noted in the benthic fauna and the climatic deterioration in the southern Atlantic (Ludwig et al., 1980).

It is interesting to note that through the Paleogene and up to the mid-Miocene there is little evidence for the development of strong vertical gradients in the oxygen isotopes. This has been interpreted as evidence for a rather small and nearly constant thermal gradient from deep to shallow water and from low to high latitude; however, there is ample evidence for changes in the benthic fauna and in patterns of carbonate dissolution and erosion through this interval. This suggests that the haline part of the thermohaline circulation played a significant role during this time. Relatively warm, salty waters can achieve nearly the same density as colder, fresher waters (much as the North Atlantic Deep Water and Antarctic Deep Water of the modern ocean). Because of the temperature and salinity effects, benthic organisms might show little difference between the two water masses in the oxygen isotope ratios incorporated in their tests. Yet there may be marked differences in the nutrient chemistry of two such water masses. With the core material now available from the South Atlantic it should be possible to map the faunal, lithologic, and isotopic indicators of these water masses through time.

SUMMARY AND CONCLUSIONS

1. As suggested by crustal magnetic anomaly patterns and igneous petrology, this section of the Walvis Ridge was initially formed at a mid-ocean ridge spreading center at an anomalously shallow elevation. The age of the basement rocks is approximately 69–71 Ma (Magnetic anomaly 31–32 time) with the deeper sites slightly younger than the sites upslope.

2. The basement is composed of basaltic pillowed and massive flows intercalated with nannofossil chalks and limestones containing a significant volcanogenic component. The major-element chemistry shows a change from quartz tholeiitic basalt at the ridge crest to olivine tholeiitic basalt down the northwestern flank. The chemistry of crestal magmas differs from that of mid-ocean ridge basalt previously recovered from the South Atlantic. Seismic sonobuoy and logging records indicate that the interlayed arrangement of basalt and sediment continues for some depth beyond the bottom of the holes, and that sediment increases with depth until true basement (Layers II, III) is reached at approximately 325 m sub-bottom.

3. The lithology of the sections is dominated by carbonate oozes and chalks. Dissolution had a marked effect on accumulation in the deeper sites, particularly during the late Miocene, Oligocene, and middle to late Eocene.

4. Volcanogenic material is common in the Maestrichtian and lower Paleocene sediments and was probably derived from sources on or near the Walvis Ridge. Continentally derived components are more easily detected at deeper sites that are more distant from the volcanic source.

5. There are six peaks in the average accumulation rate of carbonate: (a) the Upper Cretaceous; (b) the upper Paleocene–lower Eocene; (c) the basal Oligocene; (d) near the Oligocene/Miocene boundary; (e) the upper middle Miocene; and (f) the lower Pliocene. The basal Oligocene peak is not large and is seen primarily in the deeper sites. The peak at the Oligocene/Miocene boundary is large and is confined to the 23–24 Ma interval. The very peaked nature of this maximum may be an artifact of the timescale used. Other maxima range between one and a half and two times modern values and up to four times the rates of the Oligocene and mid-Eocene.

6. The peaks in carbonate accumulation appear to represent maxima in productivity. They are found in the shoalest sites, where dissolution effects should be negligible. They also appear to match peaks in the accumulation rate of fish teeth.

7. Changes in the partitioning of $\delta^{13}C$ and carbonate accumulation rates suggest a marked drop in productivity at the Cretaceous/Tertiary boundary. Through the Cenozoic sharp drops in bulk $\delta^{13}C$ appear to coincide with peak values in accumulation rates. This suggests that productivity maxima result from a realization of the productivity potential indicated by the preceding $\delta^{13}C$ maxima.

8. Dissolution followed a complex pattern through the Cenozoic. The CCD was relatively deep (~ 3500 m) during the early Paleogene and rose sharply during the mid-Eocene (when deep and surface waters were at their warmest). The CCD dropped sharply at the Eocene/Oligocene boundary; the improved carbonate preservation was seen first at shallow sites and later at deeper sites. Through the Oligocene the CCD rose, reaching its shoalest depth (~ 3500 m) in the early to middle Miocene. Near the time of Antarctic glaciation, the CCD dropped sharply and reached its present depths by the early Pliocene.

9. A mid-depth (2000–2600 m) erosion/dissolution episode affected the Angola Basin (Sites 525, 529) from late Paleocene to late Oligocene times. Another mid-depth erosional episode affected the upper Miocene of Site 529 (3000 m).

10. Accumulation rates of the coarse-grained (foraminiferal) carbonates indicate that the importance of foraminifers in carbonate production increased after the Mid-Miocene, particularly in Pliocene and younger sediments.

11. Changes in the accumulation rate of the > 63 μm fraction with depth suggest that a significant amount of dissolution occurs between the shoalest site (525; 1000 m) and the next deepest Site (526; at ~ 2500 m).

12. The effects of sediment winnowing are evidenced by a systematic downslope increase in the accumulation rate of the fine-grained carbonate. Maximum values are usually found just above the CCD. The downslope maxima in accumulation are on the order of 2 times the maximum measured at the top of the Walvis Ridge.

13. Changes in benthic fauna, stable isotopes, and/or patterns of carbonate dissolution with depth suggest

changes in the vertical structure of the deep ocean at the following times:

a) the end of the Paleocene (both benthic faunal change and onset of mid-depth erosion),

b) during the middle Eocene (rise of the CCD);

c) at the Eocene/Oligocene boundary (a sharp drop in the CCD and marked cooling of deep and surface waters);

d) near the top of the Oligocene (change in benthic fauna and cessation of mid-depth erosion);

e) in the mid-Miocene (change in oxygen isotopes and CCD associated with Antarctic glaciation);

f) in the late Miocene (reappearance of Oligocene-type elements in the benthic fauna, a possible second episode of mid-depth erosion, and a further drop in the CCD);

g) in the late Pliocene (an increase in $\delta^{18}O$ associated with the Northern Hemisphere glaciation and a change in the benthic fauna).

Although the events of the Neogene may be tied to the development of the glaciated earth, the relationship of paleoceanographic events in the Paleogene to observed changes in indicators of the deep waters are more uncertain.

REFERENCES

Alvarez, W., Arthur, M. A., Fischer, A. G., Lowrie, W., Napoleone, G., Premoli Silva, I., and Roggenthen, W. M., 1977. Upper Cretaceous–Paleocene magnetic stratigraphy at Gubbio, Italy vs. type section for the Late Cretaceous–Paleocene geomagnetic reversal time scale. *Geol. Soc. Am. Bull.*, 88:383–389.

Baker, P. E., Gass, I. G., Harris, P. G., and Le Maitre, R. W., 1964. The volcanological report of the Royal Society Expedition to Tristan da Cunha, 1962. *Phil. Trans. R. Soc. London, Ser. A*, 256: 439–575.

Berger, W. H., 1977. Carbon dioxide excursions and the deep-sea record: Aspects of the problem. *In* Andersen, N. R., and Malahoff, A. (Eds.), *The Fate of Fossil Fuel CO₂ in the Oceans:* New York (Plenum Press), pp. 505–542.

Berger, W. H., and von Rad, U., 1972. Cretaceous and Cenozoic sediments from the Atlantic Ocean. *In* Hayes, D. E., Pimm, A. C., et al., *Init. Repts. DSDP*, 14: Washington (U.S. Govt. Printing Office), 787–886.

Berger, W. H., and Winterer, E. L., 1974. Plate stratigraphy and the fluctuating carbonate line. *In* Hsu, K. J., and Jenkyns, H. C. (Eds.), *Pelagic Sediments on Land and under the Sea.* Int. Assoc. Sedimentol. Spec. Publ., 1:11–48.

Berggren, W. A., 1972. A Cenozoic time-scale—some implications for regional geology and paleobiogeography. *Lethaia*, 5:195–215.

Blow, W. H., 1969. Late Eocene to Recent planktonic foraminiferal biostratigraphy. *Proc. I Int. Conf. Planktonic Microfossils, Geneva*, 1:199–422.

Boersma, A., 1977. Cenozoic planktonic foraminifera—DSDP Leg 39 (South Atlantic). *In* Supko, P. R., Perch-Nielsen, K., et al., *Init. Repts. DSDP*, 39: Washington (U.S. Govt. Printing Office), 567–590.

_____, in press. Oligocene and other Tertiary benthic foraminifers from a depth traverse down Walvis Ridge, Deep Sea Drilling Leg 74, Southeast Atlantic. *In* Hay, W. W., Sibuet, J.-C., et al., *Init. Repts. DSDP*, 75: Washington (U.S. Govt. Printing Office).

Bolli, H. M., 1957. Planktonic foraminifera from the Oligocene-Miocene Cipero and Lengua Formations of Trinidad, B.W.I., *U.S. Nat. Mus. Bull.*, 215:91–123.

Bolli, H. M., Ryan, W. B. F., et al., 1978. *Init. Repts. DSDP*, 40: Washington (U.S. Govt. Printing Office).

Bramlette, M. N., 1958. Significance of coccolithophorids in calcium carbonate deposition. *Geol. Soc. Am. Bull.*, 69:121–126.

Burke, K. C., and Wilson, J. T., 1976. Hot spots on the earth's surface. *Sci. Am.*, 235:46–57.

Chave, A. D., 1979. Lithospheric structure of the Walvis Ridge from Rayleigh wave dispersion. *J. Geol. Res.*, 84:6840–6848.

Clague, D. A., and Bunch, T. E., 1976. Formation of ferrobasalt at East Pacific mid-ocean spreading centers. *J. Geophys. Res.*, 81: 4247–4256.

Connary, S. D., and Ewing, M., 1974. Penetration of Antarctic Bottom Water from the Cape Basin into the Angola Basin. *J. Geophys. Res.*, 79:463–469.

Detrick, R. S., and Watts, A. B., 1979. An analysis of isostasy in the world's ocean: Three aseismic ridges. *J. Geophs. Res.*, 84(no. B7): 3637–3655.

Ellis, D. B., and Moore, T. C., 1973. Calcium carbonate, opal and quartz in Holocene pelagic sediments and the calcite compensation level in the South Atlantic Ocean. *J. Mar. Res.*, 31(3):210–227.

Frey, F. A., Bryan, W. B., and Thompson, G., 1974. Atlantic Ocean floor: Geochemistry and petrology of basalts from Legs 2 and 3 of the Deep Sea Drilling Project. *J. Geophys. Res.*, 79:5507–5527.

Goslin, J., and Sibuet, J.-C., 1975. Geophysical study of the easternmost Walvis Ridge, South Atlantic: Deep structure. *Geol. Soc. Am. Bull.*, 86:1713–1724.

Heath, G. R., Moore, T. C., Jr., and van Andel, Tj. H., 1977. Carbonate accumulation and dissolution in the equatorial Pacific during the past 45 million years. *In* Andersen, N. R., and Malahoff, A. (Eds.), *The Fate of Fossil Fuel CO₂ in the Oceans:* New York (Plenum), 627–639.

Hekinian, R., 1974. Petrology of the Ninety East Ridge (Indian Ocean) compared to other aseismic ridges. *Contrib. Mineral. Petrol.*, 43: 125–147.

Hsu, K. J., LaBrecque, J. L., et al., in press. *Init. Repts. DSDP*, 73: Washington (U.S. Govt. Printing Office).

Ludwig, W. J., Krasheninnikov, V., and Shipboard Scientific Party, 1980. Tertiary and Cretaceous paleoenvironments in the southwest Atlantic Ocean: Preliminary results of Deep Sea Drilling Project Leg 71. *Geol. Soc. Am. Bull., Pt. 1*, 91:655–664.

Maxwell, A. E., von Herzen, R. P., et al., 1970. *Init. Repts. DSDP*, 3: Washington (U.S. Govt. Printing Office).

Moore, T. C., Jr., Heath, G. R., and Kowsmann, R. O., 1973. Biogenic sediments of the Panama Basin. *J. Geol.*, 81:458–472.

Morgan, J., 1971. Convection plumes in the lower mantle. *Nature*, 230:42.

_____, 1972. Plate motions and mantle convection. *Geol. Soc. Am. Mem.*, 132:7–22.

Morse, J. W., and Berner, R. A., 1972. Dissolution kinetics of calcium carbonate in sea water: II. A kinetic origin for the lysocline. *Am. J. Sci.*, 272:840–851.

Ness, G., Levi, S., and Crouch, R., 1980. Marine magnetic anomaly time scales for the Cenozoic and Late Cretaceous: A précis, critique, and synthesis. *Res. Geophys.*, 18:753–770.

Rabinowitz, P. D., and LaBrecque, J., 1979. The Mesozoic South Atlantic Ocean and evolution of its continental margins. *J. Geophys. Res.*, 84(no. B11):5973–6002.

Rabinowitz, P. D., and Simpson, E. S. W., 1979. *Results of IPOD Site Surveys aboard R/V* Thomas B. Davie: *Walvis Ridge Survey.* Lamont-Doherty Geological Observatory of Columbia University Tech. Rept., JOI Inc.

Richardson, S. H., Erlank, A. J., Duncan, A. R., and Reid, D. L., in press. Correlated Nd, Sr and Pb isotope variation in Walvis Ridge basalts and implications for the evolution of their mantle source. *Earth Planet. Sci. Lett.*

Takahashi, T., 1975. Carbonate chemistry of sea water and the calcite compensation depth in the oceans. *In* Sliter, W. V., Bé, A. W. H., and Berger, W. H. (Eds.), *Dissolution of Deep Sea Carbonates.* Cushman Found. Foram. Res., Spec. Publ., 13:11–26.

Thunell, R. C., 1982. Carbonate dissolution and abyssal hydrography in the Atlantic Ocean. *Mar. Geol.*, 47:165–180.

Thunell, R. C., Keir, R. S., and Honjo, S., 1981. Calcite dissolution: An *in situ* study in the Panama Basin. *Science*, 212:659–661.

Vail, P. R., Mitchum, R. M., Jr., Thompson, S., III, 1977. Global cycles of relative changes of sea level. *In* Payton, C. E. (Ed.), *Seismic Stratigraphy—Applications to Hydrocarbon Exploration*. Am. Assoc. Pet. Geol., Mem., 26:83–97.

Whitford, D. J., and Duncan, R. A., 1978. Origin of the Ninety East Ridge: Trace element and Sr isotopic evidence. *Carnegie Inst. Washington Yearbook*, 77:606–613.

Williams, D., Healy-Williams, N., Thunell, R., and Leventer, E., in press. Detailed stable isotope and carbonate records from the late Maestrichtian–early Paleocene section of Hole 516F, including the Cretaceous/Tertiary boundary. *In* Barker, P. F., Carlson, R. L., Johnson, D. A., et al., *Init. Repts. DSDP*, 72: Washington (U.S. Govt. Printing Office).

Wilson, J. T., 1963. Evidence from islands on the spreading of ocean floors. *Nature*, 197:536–538.

Wust, G., 1936. Das Bodenwasser und die Gliederung der Atlantischen Tiefsee. *Wiss. Ergeb. Deut. Atl. Exped.* Meteor, *1925–1927*, 6(no. 1):3–107.